Chapter C: Groundwater Flow

By Donald S. Sweetkind, Melissa D. Masbruch, Victor M. Heilweil, and Susan G. Buto

Chapter C of

Conceptual Model of the Great Basin Carbonate and Alluvial Aquifer System

Edited by Victor M. Heilweil and Lynette E. Brooks

Scientific Investigations Report 2010–5193

U.S. Department of the Interior
U.S. Geological Survey

U.S. Department of the Interior
KEN SALAZAR, Secretary

U.S. Geological Survey
Marcia K. McNutt, Director

U.S. Geological Survey, Reston, Virginia: 2011

For more information on the USGS—the Federal source for science about the Earth, its natural and living resources, natural hazards, and the environment, visit http://www.usgs.gov or call 1-888-ASK-USGS

For an overview of USGS information products, including maps, imagery, and publications, visit http://www.usgs.gov/pubprod

To order this and other USGS information products, visit http://store.usgs.gov

Suggested citation:
Heilweil, V.M., and Brooks, L.E., eds., 2011, Conceptual model of the Great Basin carbonate and alluvial aquifer system: U.S. Geological Survey Scientific Investigations Report 2010-5193, 188 p.

Contents

Figures

Tables

Conversion Factors

Inch/Pound to SI

Multiply	By	To obtain
	Length	
inch (in.)	2.54	centimeter (cm)
inch (in.)	25.4	millimeter (mm)
foot (ft)	0.3048	meter (m)
mile (mi)	1.609	kilometer (km)
	Area	
acre	4,047	square meter (m^2)
acre	0.4047	hectare (ha)
square mile (mi^2)	2.590	square kilometer (km^2)
	Volume	
gallon (gal)	3.785	liter (L)
gallon (gal)	0.003785	cubic meter (m^3)
gallon (gal)	3.785	cubic decimeter (dm^3)
cubic foot (ft^3)	28.32	cubic decimeter (dm^3)
cubic foot (ft^3)	0.02832	cubic meter (m^3)
acre-foot (acre-ft)	1,233	cubic meter (m^3)
acre-foot (acre-ft)	0.001233	cubic hectometer (hm^3)
	Flow rate	
acre-foot per year (acre-ft/yr)	1,233	cubic meter per year (m^3/yr)
acre-foot per year (acre-ft/yr)	0.001233	cubic hectometer per year (hm^3/yr)
foot per year (ft/yr)	0.3048	meter per year (m/yr)
cubic foot per second (ft^3/s)	0.02832	cubic meter per second (m^3/s)
cubic foot per day (ft^3/d)	0.02832	cubic meter per day (m^3/d)
gallon per minute (gal/min)	0.06309	liter per second (L/s)
	Hydraulic conductivity	
foot per day (ft/d)	0.3048	meter per day (m/d)
inch per day (in./d)	25.38	millimeter per day (mm/d)
	Transmissivity*	
foot squared per day (ft^2/d)	0.09290	meter squared per day (m^2/d)

Note: The conversion factors given above are for the entire report. Not all listed conversion factors will be in any given chapter of this report.

Temperature in degrees Celsius (°C) may be converted to degrees Fahrenheit (°F) as follows:

°F=(1.8×°C)+32

Temperature in degrees Fahrenheit (°F) may be converted to degrees Celsius (°C) as follows:

°C=(°F-32)/1.8

Temperature in kelvin (K) may be converted to degrees Fahrenheit (°F) as follows:

°F=1.8K-459.67

Temperature in kelvin (K) may be converted to degrees Celsius (°C) as follows:

°C=K-273.15

Vertical coordinate information is referenced to the North American Vertical Datum of 1988 (NAVD 88).

Horizontal coordinate information is referenced to the North American Datum of 1983 (NAD 83).

Altitude, as used in this report, refers to distance above the vertical datum.

*Transmissivity: The standard unit for transmissivity is cubic foot per day per square foot times foot of aquifer thickness [(ft^3/d)/ft^2]ft. In this report, the mathematically reduced form, foot squared per day (ft^2/d), is used for convenience.

Chapter C: Groundwater Flow

By Donald S. Sweetkind, Melissa D. Masbruch, Victor M. Heilweil, Susan G. Buto

The Great Basin carbonate and alluvial aquifer system (GBCAAS) study area includes a vast climatologically and geologically diverse part of the western United States. This chapter further develops the conceptual understanding of groundwater flow in the GBCAAS by (1) subdividing the study area into smaller regions of hydrographic areas (HAs) and groundwater flow systems, (2) presenting a regional potentiometric-surface map that can be used to determine generalized groundwater flow directions, (3) integrating geologic constraints along the boundaries of the HAs in the regional potentiometric-surface map, and (4) further interpreting geologic controls on the flow of groundwater. Because of the large size of the study area and sparsity of water-level data in many areas, the potentiometric-surface map depicts a simplified representation of groundwater conditions best suited for evaluating groundwater flow in a regional context.

Hydrographic Areas and Regional Groundwater Flow Systems

The GBCAAS study area comprises 165 individual HAs (pl. 1). HAs in Nevada were delineated systematically by the U.S. Geological Survey (USGS) and Nevada Division of Water Resources (NDWR) in the late 1960s (Cardinalli and others, 1968; Rush, 1968) for scientific and administrative purposes. The same system was extended into Utah, Idaho, and California during the USGS Great Basin Regional Aquifer Systems Analysis (RASA) study (Harrill and others, 1988). Generally, HA boundaries coincide with topographic basin divides; however, some divisions are arbitrary, without topographic basis (Welch and others, 2007). Most HAs represent a single watershed, including both basin fill and adjacent mountain blocks up to the topographic divide (Harrill and Prudic, 1998).

This study utilizes the naming and numbering convention for HAs used by Harrill and others (1988). While this naming and numbering convention is generally the same as the system developed by Cardinalli and others (1968), the following eight differences are noteworthy:

1. Snake Valley (HA 254 in the current study) was originally divided into three valleys by Cardinalli and others (1968): Hamlin Valley (HA196), Pleasant Valley (HA 194), and Snake Valley (HA 195).
2. Death Valley (HA 243 in the current study) is extended slightly to the southwest from the original RASA boundary to match the Death Valley regional flow system (DVRFS) study area boundary (Belcher, 2004); it is divided into two valleys by Cardinalli and others (1968): Grapevine Canyon (HA 231) and Oriental Wash (HA 232).
3. Beryl-Enterprise Area (HA 280) is referred to by Cardinalli and others (1968) as the Escalante Desert (HA 197).
4. Tenmile Creek Area (HA 48 in the current study) is referred to by Cardinalli and others (1968) as Dixie Creek-Tenmile Creek area (HA 48).
5. Great Salt Lake Desert West Part (HA 261A in the current study) is referred to by Cardinalli and others (1968) as Great Salt Lake Desert (HA 192).
6. Pilot Valley (HA 252 in the current study) is included by Cardinalli and others (1968) as part of the Great Salt Lake Desert (HA 192).
7. Grouse Creek Valley (HA 251 in the current study) is referred to by Cardinalli and others (1968) as Grouse Creek Valley (HA 190) and has a significantly different southwestern boundary.
8. Deep Creek Valley (HA 253 in the current study) is referred to by Cardinalli and others (1968) as Deep Creek Valley (HA 193).

Descriptive information for the 165 HAs is given in Appendix 2. HAs range in size from 12 mi^2 for Rose Valley (HA 199) to 4,648 mi^2 for the Great Salt Lake Desert West Part (HA 261A). The mean altitude, including both the valley and mountain blocks (up to the surface-water divide) of individual HAs ranges from 2,025 ft at Lower Moapa (HA 220) to 7,788 ft at Monitor Valley Southern Part (HA 140B). Mean annual precipitation ranges from 5 in. for Amargosa Desert, Death Valley, and Valjean Valley (HAs 230, 243, 244, respectively) to 26 in. for Cache Valley (HA 272) (PRISM, 2007).

The HAs in the GBCAAS study area were grouped previously by the Great Basin RASA study into 18 regional groundwater flow systems (Harrill and others, 1988; Harrill and Prudic, 1998). These regional groundwater flow systems primarily were based on the direction of groundwater flow across HA boundaries, the permeability of the bedrock in the mountain blocks separating the HAs, and the location of major recharge and terminal discharge areas (Harrill and Prudic, 1998). Harrill and others (1988, sheet 1) state

> *Boundaries between systems are only generally defined; some may represent physical barriers to flow such as masses of intrusive rocks and others represent ground-water divides or divisions where an area of parallel flow ultimately diverges downgradient. Again, adequate hydrologic data are needed to precisely define flow-system boundaries. For much of the Great Basin, these data are not yet available.*

Since this earlier study, one small groundwater flow system (Penoyer) was incorporated into the Death Valley System in the DVRFS study (Belcher, 2004). The current study uses the same convention as the DVRFS study and groups the HAs within the study area into 17 regional groundwater flow systems (pl. 1). The groundwater flow systems are associated with flow-system numbers that appear in parentheses after the flow-system name. The Humboldt groundwater flow system (7) within the GBCAAS is only a portion of the Humboldt groundwater flow system defined in the RASA study. Because previous studies (Harrill and others, 1988; Harrill and Prudic, 1998) show only a small amount of subsurface outflow mainly along the Humboldt River from this portion of the Humboldt groundwater flow system (7), the portion of the flow system within the GBCAAS study area is assumed to be separate from the remaining flow system that is outside the GBCAAS study area. Groundwater flow systems range in size from 282 mi^2 for the Monte Cristo Valley (23) to 18,849 mi^2 for the Great Salt Lake Desert (37) groundwater flow systems (Appendix 2).

To ensure consistency with earlier studies, the groundwater flow system boundaries defined in this study coincide with HA boundaries, though in some cases these boundaries may not define actual groundwater flow boundaries. For example, recent three-dimensional numerical modeling of groundwater flow in coupled mountain/basin terrain indicates that in moderately steep topographic settings with recharge controlled water-table altitudes (such as the eastern Great Basin), groundwater divides (a type of no-flow groundwater flow boundary) may be quite different from surface-water divides (Gleeson and Manning, 2008). Previous investigations within the study area, in fact, suggest there is substantial movement of groundwater flow across these groundwater flow system boundaries (Winograd and Pearson, 1976; Harrill and others, 1988; Belcher, 2004; Welch and others, 2007; Belcher and others, 2009). These previous findings are based on groundwater budget, geologic structure, hydraulic gradient, and geochemical mass balance evaluations.

Groundwater Movement

Groundwater movement within the study area typically occurs from higher altitude bedrock of mountains receiving recharge toward lower altitude discharge areas. Groundwater movement in mountainous terrains, such as the GBCAAS study area, occurs at local, intermediate, and interbasin scales (Toth, 1963; fig. C–1). At the local scale, groundwater moves along shallow and short flow paths, such as (1) from a high altitude area in the mountains to a nearby mountain stream or spring, or, (2) from a losing stream or canal along the alluvial fan near the edge of the basin to a lower altitude spring or evapotranspiration area. At the intermediate scale, some of the groundwater recharge originating in the mountains flows along paths of intermediate length and depth to discharge areas in the adjacent valley. Because of the relatively high permeability of many consolidated rocks within the study area, some mountain recharge also moves at the interbasin scale along deeper and longer flow paths that may cross HA boundaries to more distant discharge areas. Interbasin flow paths define groundwater basins that are larger than surface-water basins (defined by topography). Significant interbasin groundwater flow may occur through intervening mountains, particularly where recharge in the mountain block does not cause a substantial groundwater mound directly beneath the mountain block. Interbasin flow is well documented in certain conceptual models (Toth, 1963; Gleeson and Manning, 2008) and numerous field studies (Tiedeman and others, 1998; Thyne and others, 1999). Within the GBCAAS study area, interbasin flow has been suggested on the basis of (1) groundwater-budget imbalances and (or) the absence of groundwater discharge in some HAs (Stephens, 1974; Gates and Kruer, 1981; Harrill and Prudic, 1998; Welch and others, 2007), (2) isotopic studies (Winograd and Pearson, 1976; Coplen and others, 1994; Kirk and Campana, 1990; Thomas and others, 2001; Lundmark, 2007), (3) combined potentiometric gradient/geologic structure data (Belcher and others, 2009), and (4) numerical modeling (Prudic and others, 1995; Belcher, 2004).

In the GBCAAS study area, much of the recharge occurs in mountainous areas on consolidated rock, and most of the discharge occurs as evapotranspiration from basin fill. Consolidated rock and basin-fill aquifers typically are well connected hydraulically. Within the GBCAAS study area, most groundwater flow occurs in the upper basin-fill aquifer (UBFAU), upper carbonate aquifer (UCAU), and lower carbonate aquifer (LCAU) hydrogeologic units (HGUs; Chapter B of this report). Other HGUs may be local aquifers, but typically have lower permeability and more heterogeneous properties and do not transmit significant regional groundwater flow.

Groundwater movement between two locations requires both a permeable medium (aquifer) and a hydraulic gradient—a difference in hydraulic head between the two locations. The amount of groundwater flow (Q) is defined by Darcy's Law (Freeze and Cherry, 1979) as follows:

$$Q = KIA \qquad \text{(C–1)}$$

where

- K is the hydraulic conductivity of the aquifer,
- I is the hydraulic gradient, and
- A is the cross-sectional area of the aquifer.

Cross-sectional area (A) is defined as the product of aquifer thickness (b) and aquifer width (w). The degree to which an

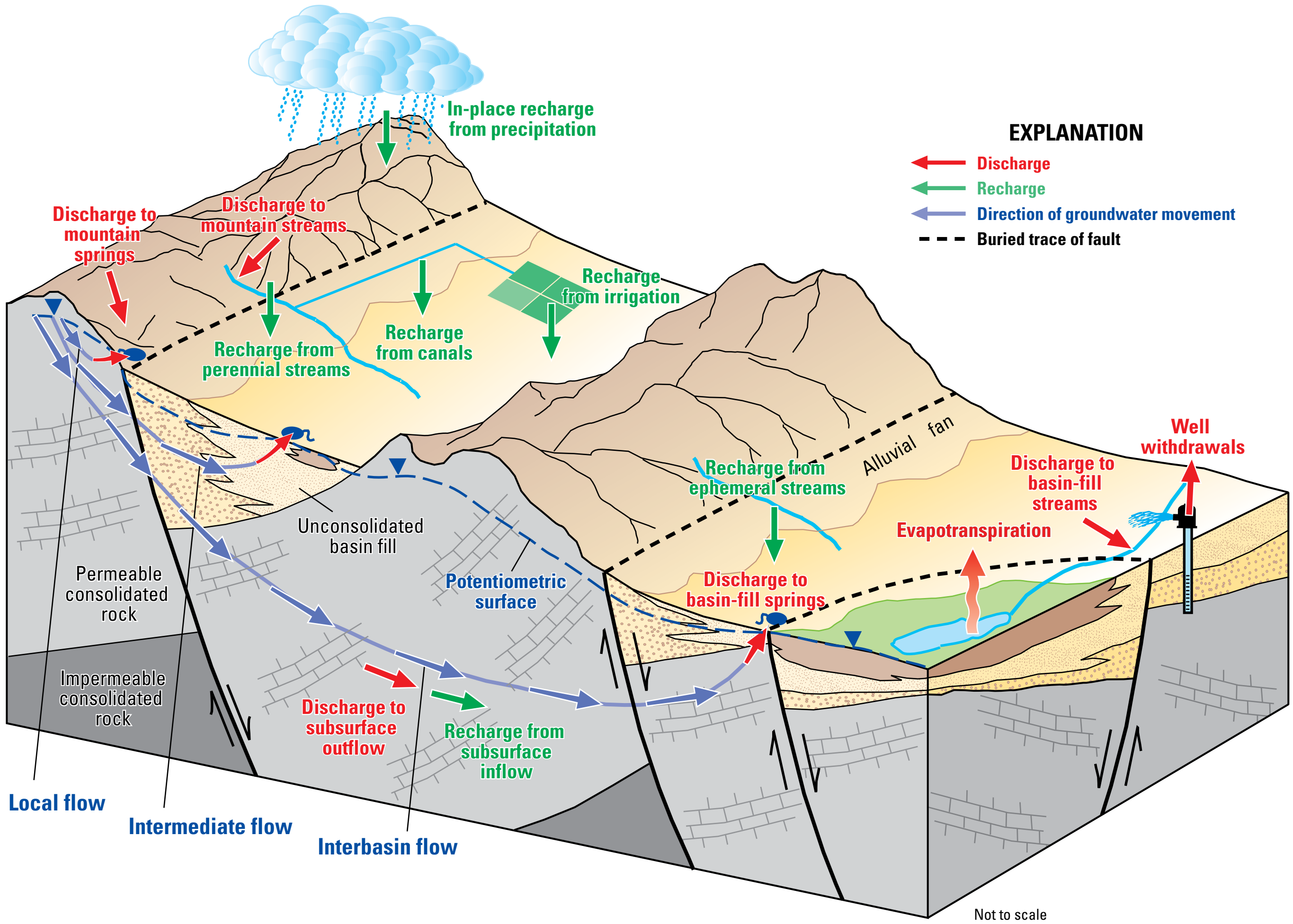

Figure C–1. Schematic diagram showing conceptualized groundwater flow in the Great Basin carbonate and alluvial aquifer system study area.

aquifer or other hydrogeologic unit is able to transmit water is often discussed in terms of its transmissivity. Transmissivity is defined as the product of the aquifer thickness and its hydraulic conductivity. Darcy's Law states that the hydraulic gradient (I) alone does not control groundwater flow; flow also depends on the hydraulic conductivity (K) and cross-sectional area (A).

Potentiometric-Surface Map

A potentiometric-surface map showing contours of equal groundwater-level altitude (pl. 2) was developed to show generalized hydraulic gradients affecting both intrabasin and interbasin groundwater flow throughout the study area. Because of the large size of the GBCAAS study area, the sparsity of hydrologic data in many of the HAs and hydrogeologic units (HGUs), and the 109-year time span (1900–2009) of the available water-level measurements, it was not within the scope of the current study to evaluate and present detailed hydraulic gradients pertaining to groundwater flow within each HA or HGU at one particular point in time. Alternatively, the groundwater conditions depicted on plate 2 are best suited for evaluating groundwater flow in a regional context, rather than addressing specific localized or transient groundwater conditions. In general, the majority of HAs within the study area have not undergone enough groundwater development to affect the potentiometric contours.

Groundwater generally follows topography and flows from areas of high land-surface altitude to areas of lower land-surface altitude, creating a general pattern of flow from mountainous areas to the Great Salt Lake Desert, the Humboldt River, the Colorado River, and Death Valley. Specifically, groundwater flows from higher to lower groundwater-level altitudes perpendicular to the potentiometric-surface contours. While not shown on the regional potentiometric-surface map of the GBCAAS study area, it is assumed that downward vertical gradients typically exist beneath recharge areas in the mountain block or along the valley margins and that upward vertical gradients exist in valley-bottom discharge areas.

The potentiometric-surface map illustrates groundwater mounding in high-precipitation and (or) less permeable mountain-block areas. Within the study area, estimated saturated hydraulic conductivity for alluvial basin-fill material is generally much higher (4.5–13 ft/d, except for mud/salt flats and playas) than consolidated bedrock (0.00016–2.6 ft/d; table A3–1). Mounding beneath the mountains is based on supporting data within the GBCAAS study area that include well water levels, along with perennial stream and spring altitudes. The concept of such mounding is consistent with earlier work. Fetter (1980) states

> *In arid regions, many rivers are fed by overland flow, interflow, and baseflow at high altitudes. As they wind their way to lower elevation, the local precipitation amounts decrease; consequently, there is less infiltration and a lower water table. There may also be a dramatic change in the depth to groundwater when a stream draining a high-altitude basin of lower permeability material flows out onto coarse alluvial materials.*

A recent modeling study of groundwater flow in mountainous terrain (Gleeson and Manning, 2008) states

> *In crystalline and other lower permeability regions, existing data suggest that water tables are often relatively close to land surface, even below high ridges. High-relief and high-water table elevations suggest that significant gravity-driven regional flow could be present in mountainous terrain.*

Data and Construction of Potentiometric-Surface Map

The potentiometric contours are based on water-level data for wells and springs compiled from the U.S. Geological Survey's National Water Information System (NWIS; Mathey, 1998) and water-level altitudes in gaged perennial mountain streams from the U.S. Geological Survey's National Hydrography Dataset (U.S. Geological Survey, 1999) for stream reaches assumed to be in hydraulic connection with recharge in the mountain block. The water-level altitudes for each well that were used as a control point for the potentiometric-surface map were averaged over the period of record for that well. Generally, the control points are coincident with the well locations, except in areas where well density is high (HAs 153, 159, 162, 212, 230, 262, 265, 266, 267, 268, 272, 273, 278, 280, 281, 282, 283, 284, 286, 287). For these HAs with high well densities, the basin fill was discretized into a grid of 2-mi^2 cells. The temporally averaged water levels for all wells within a cell were then averaged together and this water level was assigned to a single point at the center of the cell. Only nonpumping (static) water levels from wells were used to compute an average water-level altitude. Some wells were excluded from the dataset, including (1) shallow wells in mountain terrains typically less than 50 ft deep and possibly perched; (2) wells with an incorrect location in NWIS, as determined by the local name not matching the map location; (3) wells with incorrect altitude in NWIS, as determined by altitudes not matching the National Elevation Dataset (NED) altitude within the vertical accuracy of the NED (average of ± 23 ft); and (4) wells with water levels that were considered outliers when compared to other nearby control points and that may represent perched or pumping conditions. Additional exclusions were made by comparing water levels to those compiled in an unpublished database for the DVRFS study (C. Faunt, U.S. Geological Survey, written commun., 2008). If all of the water levels for a specific well were flagged in the DVRFS database with "insufficient data," "suspect," or "nonstatic level," these wells were not used as control points in the current study. Of the original 14,182 wells compiled from the NWIS database having water-level measurements, 387 were not used as control points, and only selected water-level measurements were used in 95 additional wells (Auxiliary 5). The majority of these omissions fall within the Death Valley groundwater flow system, on the basis of detailed analyses related to recent studies in this area (Belcher, 2004; Fenelon and others, 2010). A total of 13,795 wells with water-level measurements were used in constructing the potentiometric surface map (Auxiliary 6).

The potentiometric surface shown on plate 2 was generated by manually contouring the control-point data without consideration for either the depth of well penetration or the geologic formations (or HGUs) penetrated by the wells. Thus, the derived potentiometric surface emphasizes horizontal groundwater movement from recharge to discharge areas and does not depict vertical hydraulic gradients, such as localized downward vertical gradients assumed to occur in recharge areas and upward vertical gradients in discharge areas. Previous studies have published separate carbonate aquifer and basin-fill potentiometric-surface maps (Thomas and others, 1986, pls. 1 and 2; Wilson, 2007, pls. 1 and 2). The water levels in these previously published carbonate aquifer potentiometric-surface maps, however, largely were based on wells screened in the basin fill, in part owing to the scarcity of wells penetrating the deeper bedrock aquifers. The potentiometric-surface map developed for the current study, in contrast, does not distinguish wells screened within the basin fill from wells screened within the bedrock. This simplifying assumption is consistent with previous subregional potentiometric-surface maps of portions of the study area in which water levels in the shallow alluvium were assumed to be in hydraulic connection with the underlying permeable bedrock (Belcher, 2004; Wilson, 2007). The assumption is supported by groundwater altitudes from nested piezometers in Snake Valley (HA 254) that show little to no vertical gradient between basin-fill and carbonate-rock aquifers (Hugh Hurlow, Utah Geological Survey, written commun., 2008). In other areas of higher permeability bedrock overlain by basin-fill deposits, vertical nested water-level data generally are not available to confirm this assumption. In areas of low-permeability volcanic rock, such as Yucca Mountain (C. Faunt, U.S. Geological Survey, unpublished data, 2008) and Rainier Mesa (Fenelon and others, 2010), large vertical hydraulic gradients are known to exist. These steep vertical gradients may be representative of other areas with low-permeability bedrock within the GBCAAS study area, however vertically nested water-level data are not available elsewhere to confirm this.

The spring and stream altitudes used as control points for the potentiometric-surface map were considered especially important in the mountain blocks where well data are sparse. For the spring data, water-level altitudes were assumed to be equal to the spring altitude. Only single springs or groups of smaller springs (typically within 1 mi of each other), with discharge greater than 300 gal/min (about 500 acre-ft/yr), were included as control points; springs with discharge less than 300 gal/min were assumed to represent localized, perched aquifers. Stream altitudes of perennial gaining streams located within the mountain block having a baseflow of at least 300 gal/min (with a few exceptions to include streams with slightly less baseflow) were used as control points. A median altitude was calculated for each perennial mountain stream reach and used as a control point in the potentiometric-surface map. This assumes that the reach of the stream below the median altitude typically gains from groundwater discharge and is in hydraulic connection with the regional aquifer. In areas with multiple stream reaches, these median perennial stream altitudes were averaged over a 1-mi^2 grid cell and the median altitude is represented as a point at the center of the cell for the potentiometric-surface map.

The use of mountain stream altitudes as control points for the potentiometric-surface map assumes that a hydraulic connection exists between mountain-block bedrock and the rest of the groundwater system. This assumption also implies that perennial mountain-block streams are maintained by baseflow derived from discharging groundwater in the mountain block, such that the stream acts as a drain for the mountain-block aquifer. Most perennial streams occur in higher altitude mountain-block areas with higher precipitation and lower permeability bedrock. This is consistent with findings in the northern half of Great Basin National Park (Elliot and others, 2006). In such areas, groundwater mounding can be relatively steep, resulting in high-altitude water tables and local flow paths (fig. C–1) ending in discharge as baseflow to mountain streams and springs. Mounding is a function of both recharge and hydraulic conductivity. High-altitude water tables in areas such as the volcanic rocks of Rainier Mesa between Fortymile Canyon-Buckboard Mesa (HA 227B) and Yucca Flat (HA 159), and in the southern part of the San Francisco Mountains between Wah Wah Valley (HA 256) and Milford Area (HA 284), illustrate that groundwater mounding can occur in areas having low recharge rates and low hydraulic conductivity.

By use of the control points (6,444 water levels based on measurements from 13,795 wells (Auxiliary 6), 395 spring altitudes, and 2,135 gaged perennial mountain stream altitudes), as well as the characterization of groundwater flow potential across HA boundaries on the basis of geologic structure and the possible presence of recharge mounds, potentiometric contours were drawn for the entire study area at 500-ft contour intervals (pl. 2). These contours represent approximate water-level altitudes that have assumed uncertainties of at least ± 50 ft. A link to the geospatial dataset containing the control points and potentiometric contours is given in Appendix 6.

The potentiometric contours were then compared to land-surface altitudes using the U.S. Geological Survey's National Elevation Dataset (NED; U.S. Geological Survey EROS Data Center, 1999). Throughout most of the Great Basin, aquifers are generally unconfined and have water-level altitudes that are lower than land-surface altitudes. If a potentiometric altitude was greater than 100 ft above the NED altitude in areas without water-level control points, the location of the contour was adjusted until it was less than 100 ft above the NED altitude. This maximum tolerance of 100 ft above the NED altitude was chosen because of error in vertical accuracy of the NED (average of ± 23 ft) and errors associated with the computation of the control point altitudes (including both spatial and temporal averaging), which are assumed to be ± 50 ft.

Five shaded areas depicted on plate 2 represent valley areas and adjacent mountain blocks where potentiometric-surface contours are considered less certain because of the lack of water-level data. These five areas are located in (1) the northern part of the Colorado groundwater flow system centered on Jakes Valley (HA 174); (2) the western part of the Railroad Valley (30), the eastern part of the South-Central Marshes (24), and the northwestern part of the Death Valley groundwater flow systems; (3) the northeastern part of the Death Valley groundwater flow system (28); (4) the south-central part of the Colorado groundwater flow system (34) centered on Kane Springs Valley (HA 206); and (5) the southern end of the Great Salt Lake Desert groundwater flow system (37) centered on the southern parts of Snake Valley (HA 254) and Pine Valley (HA 255). While potentiometric-surface contours are drawn through these areas, the locations of these contours are less certain than in other parts of the GBCAAS study area.

Because the water-level altitudes for each well were averaged over the period of record, the potentiometric-surface map does not portray conditions during a particular season or year, but rather portrays an approximate average based on water levels spanning a period of more than 70 years. This temporal averaging approach is considered appropriate for the scope and scale of this study, with the objective of providing an overview of regional-scale groundwater flow. There are inherent uncertainties, however, in using a temporally mixed (averages computed for different periods of record) water-level data set for the development of the regional potentiometric-surface map. The majority of water-level hydrographs from the study area show no long-term monotonic trends (declining or rising water levels), but do show responses to both seasonal precipitation patterns and multiyear cycles of drought and wet periods. The use of one particular water-level measurement from a well with multiple measurement dates was not considered as representative as a temporal average, particularly for wells in fractured bedrock or along valley margins where seasonal variations can approach 100 ft. This is consistent with water-level data from wells in alpine watersheds, where seasonal water-level fluctuations approach 170 ft (Manning and Caine, 2007) and numerical modeling shows that high relief, high water-table elevations in mountainous terrain can cause significant gravity-driven regional groundwater flow (Gleeson and Manning, 2008). The maximum historical change in water level at any particular well is generally less than 100 ft. The error associated with the use of temporally averaged water levels for these wells is assumed to be consistent with, and of similar magnitude to, other simplifications and sources of inaccuracy regarding the water-level control points used to constrain the potentiometric-surface map (pl. 2).

Analysis of Potentiometric-Surface Map

Within the GBCAAS, groundwater levels and horizontal hydraulic gradients (pl. 2) typically follow topographic gradients, but with a dampened amplitude. Areas with locally steep hydraulic gradients (higher density of potentiometric contours) may indicate a decrease in transmissivity (either thinning of the more permeable zones within the aquifer or reduction in the hydraulic conductivity) and (or) relatively high groundwater flow. At the interbasin scale, groundwater flow between HAs or groundwater flow systems may occur only where a gradient exists and the intervening mountains comprise permeable rocks. The potentiometric-surface map indicates the potential for water to move in directions perpendicular to the contours. Figure C–2 conceptually illustrates three types of groundwater flow conditions at HA boundaries: (1) no-flow divides, such as beneath the Ruby and Stansbury mountains, where the modeled hydrogeologic framework indicates a low likelihood of hydraulic connection (see “Likelihood of Hydraulic Connection Across Hydrographic Area Boundaries” section below); (2) no-flow divides, such as beneath the Oquirrh Mountains, where the geology indicates a high likelihood of hydraulic connection, but groundwater mounding forms a hydraulic divide; and (3) flow across HA boundaries, such as beneath the Pequop Mountains, where the geology indicates a high likelihood of hydraulic connection and there is likely insufficient mounding to cause a hydraulic divide.

The potentiometric-surface map developed for the GBCAAS study area (pl. 2) shows that groundwater has the potential to flow across the previously defined groundwater flow system boundaries at many locations. The following list gives those locations and also gives references to previous reports indicating similar flowpaths:

1. The Grass Valley groundwater flow system (25) north to the Humboldt groundwater flow system (7);
2. The Ruby Valley groundwater flow system (33) northwest

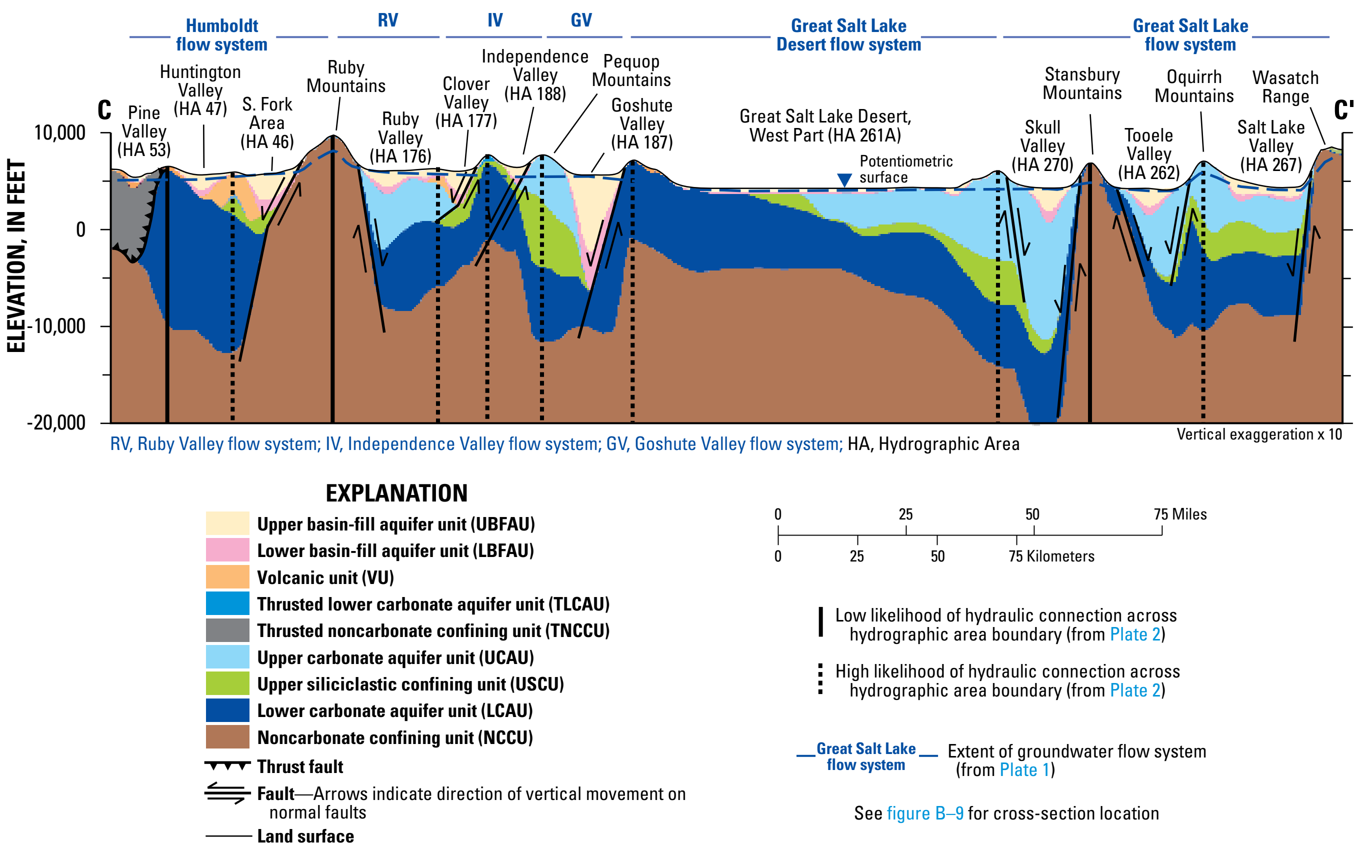

Figure C–2. Cross section showing the modeled hydrogeologic framework, potentiometric surface, and likelihood of hydraulic connections across hydrographic area boundaries and groundwater flow systems in the Great Basin carbonate and alluvial aquifer system study area.

to the Humboldt groundwater flow system (7) (fig. C–2; Thomas and others, 1986, sheet 2);

3. The Ruby Valley groundwater flow system (33) northeast through the Independence Valley groundwater flow system (32) and northern portion of the Goshute Valley groundwater flow system (35) toward the Great Salt Lake Desert groundwater flow system (37) (fig. C–2; Thomas and others, 1986, sheet 2);
4. The Diamond Valley (27) and Newark Valley (29) groundwater flow systems north to the Humboldt groundwater flow system (7);
5. The Diamond Valley (27) and Newark Valley (29) groundwater flow systems south to the South-Central Marshes (24) and Railroad Valley (30) groundwater flow systems (Thomas and others, 1986, sheet 2; Wilson, 2007, pl. 1);
6. The Monte Cristo Valley (23), South-Central Marshes (24), and Railroad Valley (30) groundwater flow systems toward the Death Valley groundwater flow system (28) (Belcher, 2004, pl. 1);
7. The Independence groundwater flow system (32) north toward the Great Salt Lake Desert groundwater flow system (37);
8. The Independence groundwater flow system (32) west through the Goshute Valley groundwater flow system (35) toward the Great Salt Lake Desert groundwater flow system (37) (fig. C–2; Thomas and others, 1986, sheet 2);
9. The northern part of the Goshute Valley groundwater flow system (35) towards the Great Salt Lake Desert groundwater flow system (37) (fig. C–2; Thomas and others, 1986, sheet 2; Wilson, 2007, pl. 1); and
10. The Great Salt Lake Desert (37), Great Salt Lake (38), and Sevier Lake (39) groundwater flow systems in eastern Nevada and western Utah toward the Great Salt Lake Desert playa and the Great Salt Lake (Thomas and others, 1986, sheet 2).

Comparisons were made between the potentiometric-surface map developed in the current study and regional potentiometric-surface maps developed for the Great Basin RASA study (Thomas and others, 1986, pls. 1 and 2), the DVRFS study (Belcher, 2004, pl. 1), and the Basin and Range carbonate-rock aquifer system (BARCAS) study (Wilson, 2007, pls. 1 and 2). In general, water-level altitudes are consistent between the maps. The main differences between the current study map and these previous regional potentiometric-surface maps are (1) the inclusion of control point altitudes of springs and gaged perennial streams thought to represent recharge mounds beneath mountain blocks and (2) having contours intersect HA boundaries perpendicularly in areas where groundwater flow between HAs is improbable because of a low likelihood of hydraulic connection on the basis of subsurface geology. In areas having high mountain-block recharge and (or) categorized as low likelihood of hydraulic connection across HA boundaries (pl. 2), flow will tend to be diverted around the mountains (instead of beneath them). For example, the existence of perennial streams within the Snake range between Spring Valley (HA 184) and Snake Valley (HA 254) in east-central Nevada and west-central Utah, and the presence of high estimated in-place recharge rates, as well as water-level altitudes of wells and large springs in and near the mountain block, suggest that a recharge mound likely exists beneath the range, as is shown in the current study potentiometric-surface map (pl. 2).

One particular difference between the current study's potentiometric-surface map and that of the RASA study (Harrill and others, 1988) is an area of high water-level altitude having a flat gradient south of Elko in the Ruby Valley (33), Newark Valley (29), and Diamond Valley (27) groundwater flow systems; the area also includes Long Valley (HA 175) of the Colorado groundwater flow system (34). The current study's potentiometric-surface map presents a new interpretation of hydraulic gradients in this area, with the potential for groundwater to flow toward four other groundwater flow systems: the Humboldt (7), Death Valley (28), Colorado (34), and Great Salt Lake Desert (37). Separating the region into four larger groundwater flow systems differs from the previous interpretation, which invoked multiple, small groundwater flow systems. In particular, Long Valley (HA 175) does not necessarily form the start of an elongated Colorado River groundwater flow system. Instead, Long Valley has the potential to receive groundwater flow from the east and contribute groundwater flow to the north and west.

Geologic Controls Affecting Groundwater Flow

Groundwater flow is affected by geology through a number of factors, including HGU thickness, geologic structures and structural zones, fault juxtaposition of HGUs with contrasting hydrologic properties, caldera formation, and regional crustal extension. Several of the areas with low hydraulic gradients on the potentiometric-surface map (pl. 2) occur in areas with large thicknesses (figs. A1–4, A1–8, and A1–9) of the most permeable HGUs (UBFAU, UCAU, and LCAU). These areas include southeast of Baker, Nevada, and west of Cedar City, Utah; the high flat area in the Ruby Valley (33), Newark Valley (29), and Diamond Valley (27) groundwater flow systems south of Elko, Nevada, that is the divide for water flowing north and south; and the flat areas in Sarcobatus Flat (HA 146), Frenchman Flat (HA 160), Penoyer Valley (HA 170), Railroad Valley-Southern Part (HA 173A), and Amargosa Desert (HA 230). Not all areas of low hydraulic gradient can be attributed to thick permeable materials. For instance, the flat area in the Great Salt Lake Desert, west of Salt Lake City, is caused by a combination of a large evapotranspiration area, flat land-surface topography, homogenous aquifer material, and little recharge.

Given the complex geologic history of the GBCAAS study area, HGUs often are disrupted by large-magnitude offset

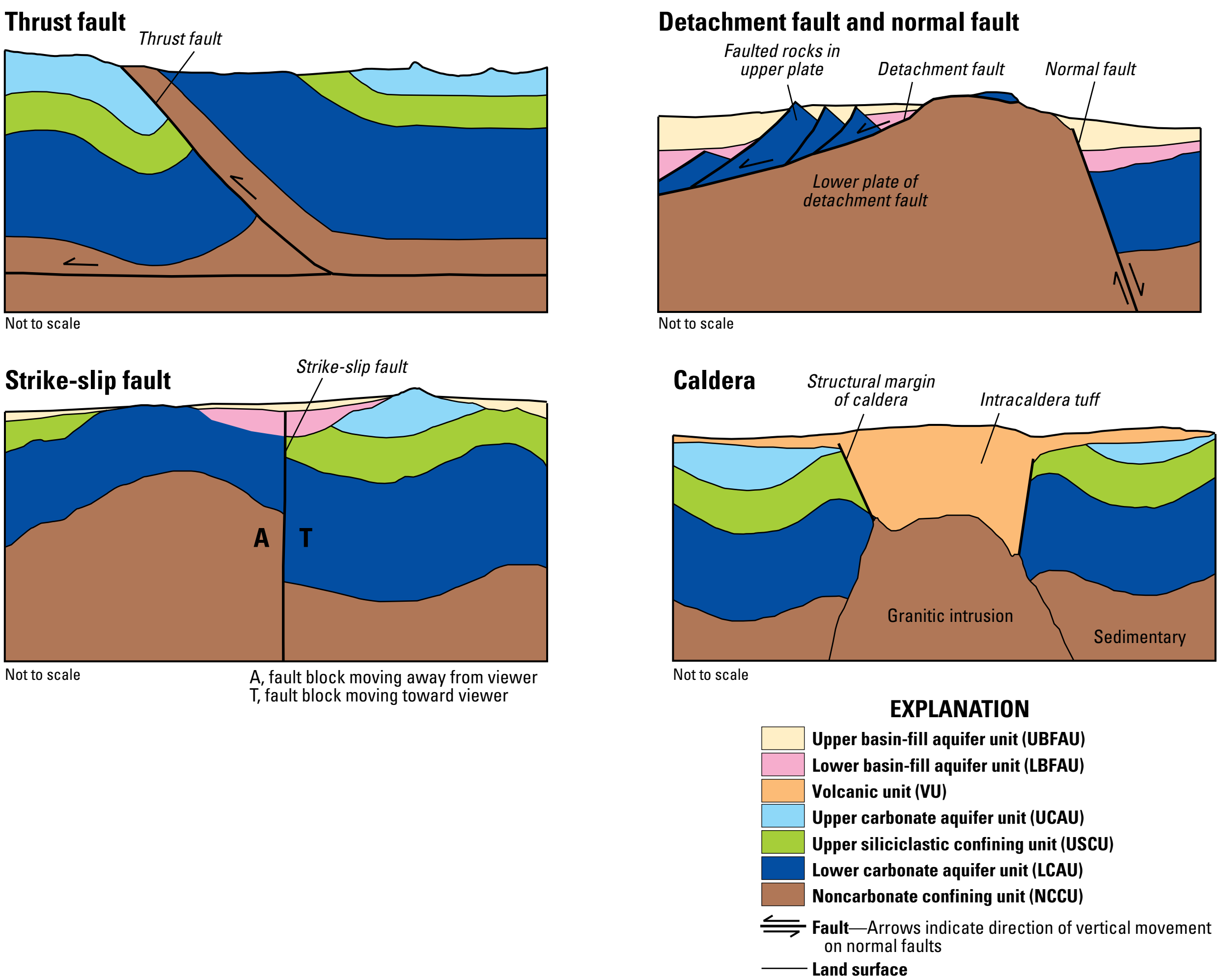

Figure C–3. Schematic diagram showing conceptualized juxtaposition of hydrogeologic units (HGUs) by different types of structures.

thrust, strike-slip, and normal faults. These geologic structures disrupt bedrock continuity (figs. C–2 and C–3) and result in a complex distribution of rocks that affect the direction and rate of interbasin groundwater flow by altering flow paths. The juxtaposition of thick, low-permeability siliciclastic-rock strata against higher permeability carbonate-rock aquifers, caused by faulting, commonly forms barriers to groundwater flow and greatly influences the shape of the potentiometric surface (Winograd and Thordarson, 1975; McKee and others, 1998; Thomas and others, 1986). Examples of this are hydraulic flow barriers ("low likelihood of hydraulic connection across an HA boundary") on the east and west sides of Northern Big Smoky Valley (HA 137B) and along the northwest edge of the Ruby Valley groundwater flow system (33) (pl. 2 and fig. C–2). Physical characteristics of fault zones may cause specific parts of the fault zone to act either as conduits or barriers to flow (Caine and others, 1996).

Structural Belts, Transverse Zones, and Mineral Belts

Thrust faults place Late Proterozoic siliciclastic rocks of the noncarbonate confining unit (NCCU) over lower Paleozoic carbonate rocks of the LCAU. In these cases, the NCCU in regional thrusts may serve to divide groundwater flow systems or divert interbasin flow. For example, thrusted NCCU on the boundary between Pine Valley (HA 53) and Huntington Valley (HA 47) locally divide groundwater flow between these HAs (pls.1 and 2). This division of flow is shown on the west end of cross section *C–C′* (fig. C–2) as the juxtaposition of thrusted noncarbonate confining unit (TNCCU) to the west and LCAU to the east; it is also shown on plate 2 as a "low likelihood of hydraulic connection." Thrust faults along the southeastern edge of the Sevier fold-and-thrust belt place lower Paleozoic carbonate rocks of the LCAU over cratonic clastic sedimentary rocks of Triassic through Cretaceous age (Armstrong, 1968; Burchfiel and others, 1992; Allmendinger, 1992; DeCelles, 2004); these rocks have been included within the UCAU (east end of section *H–H′* beneath Lower Meadow Valley Wash on fig. B–10*B*). In these cases, such as in the Muddy, Clover, and Meadow Valley mountains (pl. 1), lower permeability rocks beneath the thrust may impede downward groundwater flow from the carbonate rocks of the thrust sheet, or even force groundwater to the surface. Low-permeability siliciclastic rock in the upper plate of some thrust faults have been interpreted to cause significant diversions of groundwater flow or steep hydraulic gradients in the Death Valley region (Winograd and Thordarson, 1975; D'Agnese and others, 1997; Potter and others, 2002).

Major strike-slip faults of the Walker Lane belt (fig. B–6) occupy broad valleys in the southwestern part of the study area; these large-offset, strike-slip faults are oriented northwest and, in many cases, juxtapose different HGUs on opposite sides of the fault (fig. B–9). Detailed geologic and hydrologic studies of two of these faults, the Las Vegas Valley shear zone northwest of Las Vegas (fig. B–9; Winograd and Thordarson, 1975) and the Stateline fault system along the Nevada-California border (fig. B–9; Sweetkind and others, 2004), interpreted these faults as barriers to groundwater flow on the basis of the presence of local steep hydraulic gradients, the location of springs, and the location of the fault with respect to predominant northeast-to-southwest groundwater flow in the region. For example, there is a steep hydraulic gradient and a low likelihood of hydraulic connection along the boundary between Amargosa Desert (HA 230) and Death Valley (HA 243) (pl. 2). Geophysical investigations of strike-slip faults of the Walker Lane belt (Blakely and others, 1998; Langenheim and others, 2001) portray a structurally complex pre-Cenozoic surface adjacent to these faults, that comprise steep-sided local depressions and ridges that juxtapose HGUs in complex ways. The occurrence of springs in Pahranagat Valley (HA 209) in the Colorado groundwater flow system (34), and the southward gradient of the potentiometric surface in this vicinity (pl. 2) may be associated with northeast-striking strike-slip faults of the Pahranagat shear zone (northeast-striking faults to the south of section *G–G′*, fig. B–9).

Regional-scale transverse zones (Ekren and others, 1976; Rowley, 1998; Stewart, 1998; fig. B–6) are not well expressed in surficial outcrops, and the influence of such zones on groundwater flow patterns is largely unknown and is not readily apparent on the potentiometric-surface map. Many of the proposed zones are oriented nearly perpendicular to the long axes of current basins and ranges, however, and, as a result, may influence the rate or direction of groundwater flowing parallel to valley axes. Northwest-striking structural zones associated with major mineral belts in north-central Nevada appear to have localized mineralizing fluids periodically over geologic time (Hofstra and Cline, 2000; Emsbo and others, 2006), though the effect of this process on groundwater flow is unclear.

Calderas

The juxtaposition of contrasting lithologies at the margins of calderas affects local and regional groundwater hydrology. Structural collapse, the hallmark of caldera-forming eruptions, occurs along a generally circular system of normal faults that constitute the caldera's structural margin (fig. B–8). The lithologic discontinuity across the steeply inclined structural margin can extend to depths of several thousands of feet. Where calderas form within the carbonate rock terrain, little or no carbonate aquifer would be expected at depth beneath the caldera structure; these rocks are presumably removed during explosive caldera eruptions and intruded by subcaldera granitic rocks (fig. C–3). The structural and topographic margins of calderas juxtapose intracaldera and outflow-facies volcanic rocks. The intracaldera environment is usually filled by several thousands of feet of ash-flow tuff and interleaved landslide materials (Smith and Bailey, 1968; Lipman, 1984). Intracaldera rocks differ in their geometry and material properties from equivalent outflow rocks in that they have greater thicknesses of welded material and more complex welding zonation, greater lithologic diversity (including megabreccia and thick lava accumulations), and a greater degree of alteration. Fracture patterns in intracaldera rocks tend to be more irregular than those of outflow tuffs (Blankennagel and Weir, 1973), leading to a smaller number of connected flow paths. Outflow tuff sheets, although thinner than intracaldera tuff accumulations, have better connected fracture networks and less likelihood of significant alteration (Blankennagel and Weir, 1973). In addition to juxtaposition at the caldera margins, calderas typically are underlain by large subvolcanic granitic intrusions, which are deep, and presumably of low permeability. These intrusions may further lower permeability of rocks surrounding calderas through contact metamorphism, hydrothermal alteration, and the replacement of precaldera rocks deposited throughout the area. This is evident on plate 2 by a steep hydraulic gradient and low likelihood of hydraulic connection between Kawich Valley (HA 157) to the northwest and Emigrant Valley-Groom Lake Valley (HA 158A) to the southeast.

Extension

Regions within the GBCAAS study area where the NCCU is structurally high often are associated with Eocene-Oligocene extension and major detachment faults (fig. B–6) that juxtapose lower plate, midcrustal, medium- and high-grade metamorphic rocks of the NCCU against unmetamorphosed upper plate rocks from various HGUs (Hamilton, 1988; fig. C–3). Examples of mountain ranges with uplifted, metamorphosed NCCU include the Ruby Mountains and East Humboldt Range, the northern Snake Range, and the ranges bounding Death Valley, including the Panamint, Funeral, and Black Mountains (pl. 1). These regions are of hydrologic significance because the major detachment faults typically bring large amounts of low-permeability rocks to the surface, usually forming the highest topography in the region (Coney, 1980), and are represented as HA boundaries with a low likelihood of hydraulic connection. The low likelihood of hydraulic connection along the HA boundary between Spring Valley (HA 184) and Snake Valley (HA 254) is one such example.

Previous regional studies noted that some steep hydraulic gradients are coincident spatially with NCCU in the lower plates of major extensional detachments (Thomas and others, 1986). Previous studies of the Death Valley groundwater flow system linked exposures of relatively low-permeability NCCU with a steep hydraulic gradient along the east side of Death Valley (D'Agnese and others, 1997; Bedinger and Harrill, 2004). Large springs in Death Valley (HA 243) are located only on the flanks of the northern part of the Grapevine Mountains and the southern part of the Funeral Mountains (Steinkampf and Werrell, 2001), where relatively permeable Paleozoic carbonate rocks of LCAU are conducive to groundwater flow; large springs are absent in areas where low-permeability NCCU units are exposed by the detachment faults.

The direction and intensity of late Eocene through Holocene extension have varied both geographically and chronologically across the GBCAAS study area, creating domains of differential extension, with highly extended domains alternating with less extended domains (Gans and Miller, 1983; Wernicke and others, 1984; Smith and others, 1991; Wernicke, 1992;). Figure B–6 depicts these greatly extended zones (tan shading) separated by less extended zones (grey shading). Less extended domains preserve the entire thickness of the LCAU and UCAU within regional-scale synclines formed during Cretaceous and early Tertiary Sevier thrusting. The LCAU and UCAU within the greatly extended domains are typically complexly faulted and thinned as a result of structural disruption (Gans and Miller, 1983). Highly extended domains often have low-permeability siliciclastic rocks or metamorphic rocks of the NCCU at or near the surface (Dettinger and Schaefer, 1996). Many of these highly extended domains appear to be separated by lateral faults, which form boundaries and transfer extensional strain between differentially extended domains.

Dettinger and Schaefer (1996) compared the structural setting and distribution of rocks within various extensional domains to the location of regional groundwater flow systems within the carbonate-rock province. They concluded that regional groundwater movement in the eastern Great Basin is dominated by flow through thick sections of consolidated carbonate rock within portions of the study area that had been extended only slightly, whereas regions affected by large-magnitude crustal extension were found to be characterized by smaller, local flow systems. Portions of the Great Salt Lake Desert groundwater flow system (HAs 254, 255, 257, 258; pl. 1) fit this conceptualization, where less extended zones within LCAU (figs. B–4B and B–6) underlie those parts of the groundwater flow system that connect upgradient, recharge-dominated parts of the system with distal discharge areas (pl. 2). The region south of the Muddy River Springs (HA 219) is an example of an area where regional extension (fig. B–6) has reduced permeability. The lower permeability in the greatly extended terrains forces water to the surface at the springs instead of allowing water to continue flowing south for eventual discharge to the Virgin River or Lake Mead (pl. 1). This is also expressed in the shape of the potentiometric contours in this area, showing a coalescing of groundwater that discharges at Muddy River Springs (pls. 1 and 2). In contrast, parts of the Colorado groundwater flow system (HA 207, HA 208; pl. 1) and the Death Valley groundwater flow system (HA 160, HA 161; pl. 1), known to be underlain by thick sections of consolidated carbonate rock, fall within greatly extended zones (fig. B–6). In these cases, lack of correspondence between extensional domain and the location of regional groundwater flow systems is, in part, a result of differences in the mapped extent of greatly extended regions used by Dettinger and Schaeffer (1996) and those shown in figure B–6. The lack of correspondence may result from the effects of other geologic factors, such as the inferred enhanced permeability north of the Las Vegas Valley shear zone (fig. B–7).

High-angle normal faults associated with younger basin-and-range style extension can have sufficiently large stratigraphic offset such that HGUs with contrasting hydrologic properties are juxtaposed across the fault. These faults disrupt aquifer continuity (fig. C–3) and may alter groundwater flow paths. Interbasin southwest-flowing groundwater in consolidated carbonate rocks is forced to the surface at Ash Meadows, in the eastern Amargosa Desert (HA 230; pl. 1), likely because the LCAU here is juxtaposed against low-permeability basin-fill materials of the lower basin-fill aquifer unit (LBFAU) and UBFAU across a normal fault (Winograd and Thordarson, 1975); Dudley and Larsen, 1976). Winograd and Thordarson (1975) interpreted a distinct gradient across this fault on their detailed potentiometric surface; at the regional scale, however, the gradient across the fault is not apparent (pl. 2).

Faults as Hydrogeologic Features

Many brittle fault zones contain a narrow core of fine-grained, relatively low-permeability gouge that is the locus of fault displacement (Caine and others, 1996). The core zone can be flanked by damage zones, a network of subsidiary small faults and fractures that enhance secondary permeability (Caine and others, 1996; Caine and Forster, 1999). In many cases, the core zone reduces permeability relative to that of the original rock or the surrounding damage zone as a result of progressive grain-size reduction, formation of clay minerals, and mineral precipitation during fault motion. Low-permeability fault cores potentially restrict fluid flow across the fault, whereas the damage zone may conduct groundwater flow parallel to the fault zone. The width of the low-permeability core zone is commonly 1.8 to 3.3 ft for high-angle normal faults in volcanic rocks at Yucca Mountain (pl. 1) and in carbonate rocks near the Nevada Test Site (fig. A–1). For these normal faults, the surrounding more permeable damage zones vary in width from about 30 to 300 ft. Dettinger (1989) reported enhanced transmissivities in normal-faulted carbonate rocks, as measured in wells drilled for the U.S. Air Force's MX missile-siting program in Coyote Spring Valley, Nevada (HA 210; pl. 1); these transmissivities are 20–40 times those measured in relatively undeformed carbonates near the Nevada Test Site (fig. A–1), and likely occur in a broad fault-related damage zone. Certain springs, such as those in central White River Valley (HA 207; pl. 1), are associated with faults, but the faults are aligned with the inferred direction of groundwater flow. It is possible, in these cases, that permeable damage zones along the fault could enhance flow.

Strike-slip faults within the GBCAAS study area are typically buried beneath alluvial cover, obscuring any direct observations of the fault core zone within these structures. In other areas where well-exposed, large-displacement, strike-slip faults have been studied, they have been characterized by a continuous, low-permeability core zone (Chester and Logan, 1986). Flow barriers along strike-slip faults, though effective locally, may be regionally discontinuous. Chester and Logan (1986), for example, noted considerable variations in the thickness of the core zone (about 0.2 to 3 ft) along an inactive strand of the San Andreas Fault. Thus, it seems likely that core zones could become irregular and discontinuous locally, resulting in a discontinuous groundwater flow barrier.

The hydrologic influence of regional fault zones has been shown numerically to be governed, at least in part, by the relative hydraulic conductivities of the mountain block, valley-fill, and fault zone, and illustrates the control exerted by regional faults in basin-and-range settings with overlying alluvium (Folch and Mas-Pla, 2008). The hydrologic influence of large-offset normal faults appears to be variable in the GBCAAS study area. In some cases, large-offset normal faults correspond to the locations of substantial groundwater discharge, and the faults may be interpreted to affect groundwater flow by impeding lateral flow and enhancing upward flow. Elsewhere, groundwater flow appears to pass directly across normal faults. Differences in water levels and water chemistry across faults in the Yucca Mountain area (pl. 1) provide evidence that some normal faults in volcanic rocks impede cross-fault flow (Luckey and others, 1996), acting as barriers and compartmentalizing the groundwater flow system. In contrast, interbasin groundwater flow has been suggested on the basis of potentiometric contours (Harrill, 1982) that pass unaffected directly across a normal fault bounding the eastern side of the Nopah Range to the west of Pahrump Valley (HA 162; pl. 1). Few data are available, however, to define the gradient to the west of the Nopah Range. Springs in Pahrump Valley discharge where LCAU is juxtaposed against LBFAU and UBFAU, even though no fault has been defined in the area. Similarly, several studies have inferred interbasin groundwater flow to the south of the Snake Range (HA 184 and 254, pl. 1) on the basis of water-budget considerations (Harrill and others, 1988; Welch and others, 2007). In this case, generally west-to-east flow must cross discontinuous north-striking normal faults bounding each side of the uplifted carbonate rocks of the Limestone Hills at the south end of the range, suggesting that these faults do little to impede interbasin flow. From data presented in Chapter D of this report, water-budget considerations based on new recharge estimates do not require interbasin flow in this area, although the potential does exist (pl. 2).

Aquifer Storage Volumes

Estimating groundwater storage is helpful for evaluating regional groundwater resources. Groundwater within the GBCAAS study area is stored within the saturated pore spaces (including both primary and fracture porosity) of both unconsolidated and consolidated hydrogeologic units. This stored groundwater is the initial source of water to a pumped well, which is later replaced by water from other sources after a new equilibrium is established within the aquifer. For a given withdrawal rate, a relatively large amount of available storage in the vicinity of the aquifer will result in less substantial drawdown effects (declining water levels, aquifer compaction, and land subsidence) and a longer lag time before re-equilibration to this stress is established, and capture of natural discharge or recharge sources occurs. The magnitude of water-level decline and (or) recovery is dependent upon aquifer storage properties: specific yield under water-table conditions and storage coefficient under confined conditions. Specific yield is typically less than the porosity of saturated sediments because some of this water is tightly bound in the pore spaces and cannot be removed under gravity drainage. A recently published groundwater resources evaluation within the study area (Welch and others, 2007) estimated groundwater storage volumes assuming a constant 100-ft decline throughout both basin-fill and adjacent consolidated rock. Within the larger GBCAAS study area, both the extent and magnitude of future water-level declines, and whether such declines would occur under confined or unconfined conditions, are unknown. Also, the storage properties of the carbonate HGUs are assumed to be much smaller and less certain than those of volcanic and basin-fill HGUs because fewer modeling studies and multiple-well aquifer tests have been done. The approach used in the current study was to estimate the total quantity of water stored in only the volcanic and basin-fill deposits. The following estimates represent the total volume of groundwater that could potentially be removed from volcanic and basin-fill units within the GBCAAS study area under unconfined conditions. These stored volumes should not be considered usable storage since it is highly unlikely that any volcanic or basin-fill HGU would undergo such complete drainage. Furthermore, the storage volumes presented here should not be considered analogous to groundwater availability within the GBCAAS study area.

Groundwater availability, in contrast, is generally considered in the context of groundwater sustainability, defined by Alley and Leake (2004):

> *as the development and use of ground water resources in a manner that can be maintained for an indefinite time without causing unacceptable environmental, economic, or social consequences.*

The estimated total storage volumes presented here, therefore, are only useful for illustrating differences in stored volumes of groundwater between HGUs in the 17 individual groundwater flow systems.

To calculate storage quantities, the aquifer volumes (below the water table) of each Cenozoic HGU (volcanic unit [VU], LBFAU, and UBFAU) were first calculated. Volumes were not determined for the older LCAU, UCAU, upper siliciclastic confining unit (USCU) and NCCU HGUs. The volumes of Cenozoic sediments were calculated on the basis of thicknesses of these units in the three-dimensional hydrogeologic framework (Chapter B of this report). The altitude used to calculate the volumes is the top of the surficial unit, or the altitude of the potentiometric surface (pl. 2) if the potentiometric surface is below land surface. Unlike the BARCAS study (Welch and others, 2007), playa deposits were not mapped separately from other basin-fill deposits and, therefore, were not subtracted from total basin-fill volumes. The estimated aquifer volumes are 1.06 x 10^{15} ft^3, 1.32 x 10^{15} ft^3, and 2.36 x 10^{15} ft^3 for VU, LBFAU, and UBFAU, respectively, within the GBCAAS study area.

The estimated total volume of water stored in these three Cenozoic aquifers was calculated by multiplying their respective aquifer volumes by ranges of previously published specific-yield values for Cenozoic deposits within the study area. These calculated volumes are hypothetical and should be used only for comparing groundwater storage volumes across the 17 groundwater flow systems; these volumes are much larger than could potentially be recovered. Specific-yield values (representing unconfined conditions) were used, rather than confined specific-storage values, because the estimates are for total volume of water stored. Specific storage would be applicable only for calculating groundwater extraction under confined conditions, not accounting for actual drainage of soil pores (Freeze and Cherry, 1979, p. 61).

A median specific-yield value of 0.03 was used for calculating water storage in the VU. This was based on reported values from multiple-well aquifer tests (table C–1), including an arithmetic mean of 0.03 from 10 aquifer tests conducted in a variety of tertiary volcanic rocks in and around the Nevada Test Site of the Death Valley (28) groundwater flow system, a value of 0.04 from an aquifer test conducted in fractured welded tuffs at the J–12WW Area 25 well in Fortymile Canyon-Jackass Flats (HA 227A) on the Nevada Test Site, and a value of 0.01 from an aquifer test conducted in volcanic rocks at the Tahoe-Reno Industrial Center in Storey County, Nevada. Although the latter test was outside of the GBCAAS study area, it is considered representative of the less fractured volcanic rocks that are present in many parts of the study area, such as zone 2 of the VU shown in figure B–4D.

Table C–1. Previously reported estimates of specific yield for Cenozoic hydrogeologic units within the Great Basin carbonate and alluvial aquifer system study area.

[HGU, hydrogeologic unit; HA, hydrographic area; VU, volcanic unit; LBFAU, lower basin-fill aquifer unit; UBFAU, upper basin-fill aquifer unit; <, less than; >, greater than; ft, feet]

Area name	Specific yield	Type of material	Pertinent HGU	Analysis type	Report	Comment
Fortymile Canyon-Jackass Flats (HA 227A)	0.04	Fractured welded tuffs	VU	Aquifer testing	http://nevada.usgs.gov/water/AquiferTests/j12ww.cfm?studyname=j12ww, accessed on 01/28/2010	J-12WW Area 25 well on the Nevada Test Site.
Nevada Test Site area of Death Valley groundwater flow system (28)	0.03	Tertiary volcanic rocks	VU	Aquifer testing	Belcher and others, 2001	Reported arithmetic mean of 0.03 based on 10 aquifer tests with values ranging from 0.001 to 0.20.
Tahoe-Reno Industrial Center (outside study area)	0.01	Less-fractured volcanic rocks	VU	Aquifer testing	http://nevada.usgs.gov/water/AquiferTests/tracy_W36-Center.cfm?studyname=tracy_W36-Center, accessed on 01/28/2010	
Frenchman Flat (HA 160)	0.21	Unconsolidated basin-fill sediments	LBFAU, UBFAU	Aquifer testing	http://nevada.usgs.gov/water/AquiferTests/rnm-2s.cfm?studyname=rnm-2s, accessed on 01/28/2010	Well RNM-2S.
Snake Valley (HA 254)	0.15	Unconsolidated basin-fill sediments	LBFAU, UBFAU	Aquifer testing	http://nevada.usgs.gov/water/AquiferTests/snake_valley_n.cfm?studyname=snake_valley_n, accessed on 01/28/2010	Reported range of 0.12 to 0.18 for well (C-20-19)19dcd-1.

Table C–1. Previously reported estimates of specific yield for Cenozoic hydrogeologic units within the Great Basin carbonate and alluvial aquifer system study area.—Continued

[HGU, hydrogeologic unit; HA, hydrographic area; VU, volcanic unit; LBFAU, lower basin-fill aquifer unit; UBFAU, upper basin-fill aquifer unit; <, less than; >, greater than; NC, not calculated; ft, feet]

Area name	Specific yield	Type of material	Pertinent HGU	Analysis type	Report	Comment
Cedar City Valley (HA 282)	0.20	Gravel	LBFAU, UBFAU	Aquifer testing	Bjorklund and others, 1978	Estimated on the basis of recovery of pumped well (C-35-10)18cca-1 (Bjorklund and others, 1978, table 4).
Milford Area (HA 284)	0.20	Coarser sediments	LBFAU, UBFAU	Aquifer testing	Mower and Cordova, 1974	Minimum value; could be as high as 0.40 for fine-grained materials.
Southern Utah and Goshen Valleys (HA 265)	0.06	Cemented sediments, gravel, sand, silt, clay	LBFAU, UBFAU	Field and lab studies	Cordova, 1970; Brooks and Stolp, 1995	Weight-based mean calculated by Brooks and Stolp of six classes (0.25, 0.05, 0.25, 0.05, 0.03, 0.01) listed in Cordova p. 56.
Deep Creek Valley (HA 253)	0.10	Sand and gravel intercalated with clay	LBFAU, UBFAU	Estimated from coarseness correlation	Hood and Waddell, 1969	On the basis of specific yield of 0.2 to 0.3 for permeable layers, which only comprise 20 percent of saturated section.
Ogden Valley (HA 268)	0.10	Unconsolidated basin-fill sediments	LBFAU, UBFAU	Estimated from coarseness correlation	Avery, 1994	
Juab Valley (HA 266)	0.15	Unconsolidated basin-fill sediments	LBFAU, UBFAU	Numerical model	Thiros and others, 1996	Area-based mean from three zones of calibrated numerical model (0.05 for fine-grained, 0.10 for medium-grained, and 0.20 for coarse-grained sediments).
Salt Lake Valley (HA 267)	0.15	Unconsolidated basin-fill sediments	LBFAU, UBFAU	Numerical model	Lambert, 1995	On the basis of calibrated specific yield for model layers 1 and 2.
Cache Valley (HA 272)	0.20	Unconsolidated basin-fill sediments	LBFAU, UBFAU	Numerical model	Kariya and others, 1994	On the basis of visual weighting of five zones from 0.01 to 0.30
Beryl-Enterprise Area (HA 280)	0.17	Fine-to-coarse unconsolidated sediments	LBFAU, UBFAU	Numerical model	Mower, 1982	On the basis of visual weighting of five zones from <0.05 to > 0.20
Cedar City Valley (HA 282)	0.05	Unconsolidated basin-fill sediments	LBFAU, UBFAU	Numerical model	Brooks and Mason, 2005	Area-based mean from two zones of calibrated numerical model (0.04 for finer-grained and 0.07 for coarser-grained deposits)
Pavant Valley (HA 286)	0.25	Finer grained silt and clay below 4,800 ft	LBFAU, UBFAU	Numerical model	Holmes and Thiros, 1990	Median of 0.20 used for finer grained silt and clay below 4,800 ft and 0.30 used for coarser-grained sand and gravel above 4,800 ft

A specific-yield value of 0.15 was used for calculating water storage in the LBFAU and UBFAU. This value is a median value derived from 13 previously reported studies having values that ranged from 0.05 to 0.25 for unconsolidated basin-fill deposits (table C–1). These studies included aquifer testing, field and lab studies, coarseness correlations, and calibrated numerical groundwater flow models. Previously reported estimates of specific yield include 0.20 to 0.25 from aquifer testing, 0.06 from field and lab studies, 0.10 from coarseness correlations, and 0.05 to 0.25 from calibrated numerical models. The median specific-yield value of 0.15 used in the current study is the same as the specific-yield value of 0.15 used for unconfined basin-fill deposits in the BARCAS study (Welch and others, 2007).

Multiplying these estimated values of specific yield of 0.03 for VU and 0.15 for LBFAU and UBFAU by their respective aquifer volumes, the estimated volumes of water stored within the Cenozoic aquifer units within the GBCAAS are 7.3 x 10^8 acre-ft, 4.5 x 10^9 acre-ft, and 8.1 x 10^9 acre-ft for VU, LBFAU, and UBFAU, respectively. Storage volumes in each of the Cenozoic HGUs for each groundwater flow system are shown on figure C–4. Estimated quantities of water stored in the VU range from 1.2 x 10^3 acre-ft to 2.2 x 10^8 acre-ft. Estimated water storage for LBFAU ranges from 1.0 x 10^7 acre-ft to 7.2 x 10^8 acre-ft. Estimated quantities of water stored in the UBFAU range from 2.0 x 10^7 acre-ft to 1.2 x 10^9 acre-ft. The smallest storage volumes are located in the Mesquite Valley groundwater flow system (36), while the largest storage volumes are located in the Death Valley groundwater flow system (28).

Likelihood of Hydraulic Connection Across Hydrographic Area Boundaries

The distribution of aquifers and confining units along HA boundaries is a principal control on interbasin groundwater flow in the study area. The occurrence and juxtaposition of aquifers and confining units in these areas must be understood to assess the geologic controls on the relative potential for groundwater flow across these boundaries. Significant groundwater flow across HA boundaries is possible only where the rocks connecting the hydrographic areas have sufficient permeability.

To assess the geologic controls on the likelihood of hydraulic connections across HA boundaries, the regional stratigraphic and structural features described previously were summarized into 14 general subsurface geologic configurations that result in differing likelihoods of hydraulic connection across HA boundaries (table C–2). Each of the

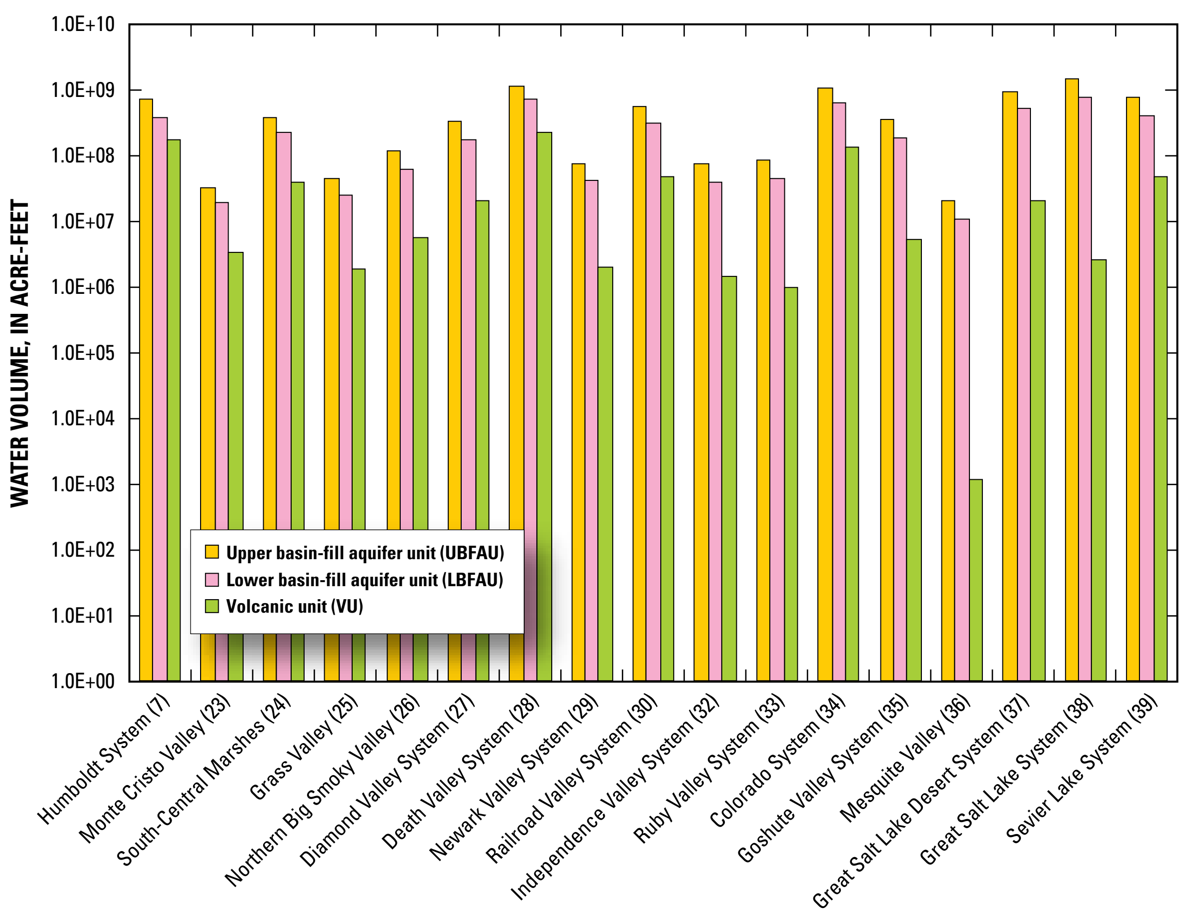

Figure C–4. Estimated volume of water stored within Cenozoic hydrogeologic units in the 17 groundwater flow systems of the Great Basin carbonate and alluvial aquifer system study area.

Table C–2. Likelihood of hydraulic connection across hydrographic area boundaries within the Great Basin carbonate and alluvial aquifer system study area.

[HGUs, hydrogeologic units; NCCU, noncarbonate confining unit; USCU, upper siliciclastic confining unit; TNCCU, thrusted noncarbonate confining unit; UCAU, upper carbonate aquifer unit; LCAU, lower carbonate aquifer unit; VU, volcanic unit; LBFAU, lower basin-fill aquifer unit; UBFAU, upper basin-fill aquifer unit; ft, feet; 3-D, three-dimensional; HA, hydrographic area; NV, Nevada; CA, California; UT, Utah ; >, greater than]

Likelihood of hydraulic connection across HA boundary	HGUs primarily responsible for geologic condition at boundary	Geologic rationale for classification
Low	NCCU	NCCU near (within about 300 ft) or at land surface, on the basis of 3-D framework. Unit assumed to project to great depths below any outcrop exposure. Included NCCU exposures from surface geologic map in places where 3-D framework did not exactly replicate the geologic map. Ignored small inliers of permeable units surrounded by NCCU.
Low	USCU	USCU near (within about 250 ft) or at land surface and unit greater than about 800 ft thick, on the basis of 3-D framework. Included selected USCU exposures from geologic map in places where unit thickness was less than about 800 ft where dip of the unit increases the cross-sectional area of the unit at the HA boundary so that unit could still function as a geologic barrier.
Low	TNCCU	HA boundaries that are parallel to thrust faults and TNCCU, such that water in Paleozoic rocks would not be expected to cross the thrust fault. For the purposes of potentiometric surface interpretation, included thrust faults from the central Nevada thrust belt and the Sevier thrust belt that were not explicitly included in the 3-D framework.
Low	Not related to a specific HGU	HA boundaries within structurally disrupted areas where local extreme extension thins or disrupts Paleozoic carbonate rocks, such that a continuous carbonate aquifer is unlikely. Includes portions of the Grant Range, northern part of the Snake Range, Egan Range, and Mormon Mountains.
Low	TNCCU	Presence of thrusted deep-water assemblages in the upper plate of the Roberts Mountain allocthon. Includes siliceous chert and limestone assemblages of the Vinini and Valmy Formations in the vicinity of Elko and Battle Mountain, NV. These units are attributed as TNCCU in the 3-D framework and are expected to be generally low-permeability rocks.
High	LCAU and UCAU	LCAU or UCAU near (within about 150 ft) or at land surface and unit greater than about 800 ft thick, on the basis of 3-D framework. Included narrow basin-fill valleys that were flanked by carbonate-rock mountain ranges where carbonate bedrock could reasonably be inferred at depth beneath valley.
High	VU	Thick (>250 ft) ash-flow tuffs overlying permeable carbonate bedrock. Ash-flow tuffs expected to support well-developed fracture networks and be moderately permeable local to subregional aquifers.
High	LBFAU and UBFAU	Areas of Cenozoic basin fill where the LBFAU is interpreted to be either ash-flow tuff or prevolcanic sedimentary rock, and the UBFAU is interpreted to be either coarse-grained younger sediment or exposures of prevolcanic sedimentary rocks that exist in the shallow part of the basin.
Uncertain	VU	Intracaldera volcanic rocks. Thick sequences of highly heterogeneous volcanic rocks (including welded and nonwelded tuff, lava flows, volcanic breccias, and nonvolcanic megabreccia deposits) that are bounded by the caldera structures. This unit overlies intrusive rocks of the NCCU inferred to be present at depth within calderas; unit has potential to be hydrothermally altered.
Uncertain	VU	Volcanic rocks, mainly ash-flow tuffs, of variable thickness that overlie impermeable bedrock. Common in Esmeralda County, NV, near Lake Mead in the southern part of Clark County, NV, and in San Bernardino County, CA.
Uncertain	VU	Highly variable volcanic rock overlying bedrock that has variable or uncertain permeability. Examples include local accumulations of rhyolite lava flow, such as at the southern end of Butte Valley, NV, or intervals of thin welded ash-flow tuff interbedded with nonwelded tuff.

Table C–2. Likelihood of hydraulic connection across hydrographic area boundaries within the Great Basin carbonate and alluvial aquifer system study area.—Continued

[HGUs, hydrogeologic units; NCCU, noncarbonate confining unit; USCU, upper siliciclastic confining unit; TNCCU, thrusted noncarbonate confining unit; UCAU, upper carbonate aquifer unit; LCAU, lower carbonate aquifer unit; VU, volcanic unit; LBFAU, lower basin-fill aquifer unit; UBFAU, upper basin-fill aquifer unit; ft, feet; 3-D, three-dimensional; HA, hydrographic area; NV, Nevada; CA, California; UT, Utah]

Likelihood of hydraulic connection across HA boundary	HGUs primarily responsible for geologic condition at boundary	Geologic rationale for classification
Uncertain	Modification of VU, LCAU, or UCAU	Mineral deposits that are associated with hydrothermal alteration and mineralization at a scale large enough to potentially disrupt the regional aquifer systems. Mainly associated with copper porphyry systems and epithermal and hot-spring precious-metal systems. Deemed important where mineralizing system intruded otherwise permeable carbonate rocks, such as at Bingham Canyon, UT, or Battle Mountain, NV. Where the mineralizing system overprints lower-permeability rocks, such as at Tintic, UT, HA boundaries were not modified from their original classification based on rock type.
Uncertain	LBFAU and UBFAU	Areas where the LBFAU, the UBFAU, or both units were fine-grained or had a large volcanic ash component.
Uncertain	NCCU	Areas where zones of closely spaced normal faults may enhance permeability of otherwise low-permeability rocks. Examples include seismogenically active faults cutting granites of the Slate Range near Lida Valley and Clayton Valley, Esmeralda County, NV.

14 subsurface geologic configurations is determined by the permeability and cross-sectional area of the HGUs and (or) geologic structures at an HA boundary. The subsurface geology at HA boundaries was interpreted primarily by evaluating vertical, irregularly bending cross-section views of the three-dimensional hydrogeologic framework model (described in Chapter B and Appendix 1) for altitude, thickness, and relative juxtaposition of specific HGUs.

Interpretation of the subsurface geology relative to the likelihood of hydraulic connection across HA boundaries primarily was based on the presence of specific HGUs or juxtaposition of HGUs with contrasting hydraulic conductivity. The degree of structural disruption at the boundary is considered an important, but secondary, control. Structural disruption may be considered as a boundary condition where closely spaced high-angle normal faults disrupt a relatively broad region and where carbonate-rock aquifers (UCAU and LCAU) are highly faulted and disrupted in the upper plates of low-angle normal faults. Because data are lacking, however, the likelihood of hydraulic connection across HA boundaries (table C–2) does not incorporate the effects of individual faults as distinct hydrologic entities. For example, the analysis omits potential effects of low-permeability, clay-rich fault core zones, fractured and potentially more permeable zones that might be located adjacent to the fault core, or strata-bound fractured intervals in volcanic or carbonate rocks.

For each of the 14 general subsurface geologic configurations (table C–2), the likelihood of hydraulic connection across HA boundaries was summarized by assigning portions of HA boundaries to one of three likelihoods (low, high, or uncertain) of hydraulic connection across the boundary (pl. 2): (1) low—relatively impermeable consolidated rock occurs at depth that inhibits groundwater flow (solid lines on plate 2), (2) high—permeable consolidated rock or basin fill occurs at depth that permits groundwater flow (dashed lines on plate 2), or (3) uncertain—the permeability of the consolidated rock or basin fill is highly variable, such that the groundwater flow potential across HA boundaries is uncertain (double lines on plate 2).

The likelihood of hydraulic connections across HA boundaries varies throughout the study area (pl. 2). HA boundaries with low likelihood of hydraulic connection (table C–2) include (1) exposures of NCCU associated with metamorphic core complexes and with other large-offset normal faults (HAs 176 and 230; pl. 1); (2) areas of thick USCU, such as thick sections of Diamond Peak Formation and Chainman Shale in north-central parts of Nevada (HAs 174 and 175; pl. 1) and at the Nevada Test Site (HA 159; pl. 1); (3) local areas where thrusted Late Proterozoic siliciclastic rocks of unit TNCCU are extensive (HA 162; pl. 1); and (4) regions of low-permeability rocks associated with the Roberts Mountains thrust belt (HAs 137B and 138; pl. 1) in the northwestern part of the study area (fig. B–5). HA boundaries with high likelihood of hydraulic connection include (1) those underlain by thick sequences of consolidated carbonate rock HGUs LCAU and UCAU (HAs 160, 161, 168, 208, 209, and 210; pl. 1), generally corresponding to the central carbonate corridor described by Dettinger and others (1995); (2) those underlain by welded ash-flow tuffs overlying permeable bedrock, typically associated with outflow tuffs that surround the major caldera complexes (HAs, 146, 150, 156, 227A, and 228; pl. 1); and (3) those underlain by permeable basin fill, especially in the Humboldt River drainage (HAs 43, 45, and 48; pl. 1) in the northwestern part of the study area (fig. A–1). HA boundaries with an uncertain likelihood of hydraulic connection include (1) accumulations of volcanic rocks (VU) that are heterogeneous (HAs 204 and 221; pl. 1) or that overlie impermeable bedrock (HAs 144 and 147; pl. 1); (2) areas where permeability may be modified as the result of hydrothermal alteration and mineralization (HA 267; pl. 1) or by the presence of structures; and (3) areas where the lower or upper basin fill (LBFAU or UBFAU) have variable properties.

Limitations

The following are several limitations that should be considered when utilizing the information presented in Chapter C:

- The objective of the potentiometric-surface contours depicted on plate 2 is to illustrate the general directions of horizontal groundwater flow within the GBCAAS study area. Because of its large regional extent and the 500-ft contour intervals, this map is not suitable for evaluating detailed flow conditions at the sub-HA level.
- Plate 2 was developed without consideration for vertical flow between HGUs because of a general lack of water-level data to accurately quantify vertical hydraulic gradients in most of the GBCAAS study area. While not displayed on plate 2, there is the possibility that significant vertical gradients between HGUs exist in parts of the study area, typically in lower permeability bedrock. Detailed water-level data from volcanic aquifers, such as those at Rainier Mesa and the Nevada Test Site (Fenelon and others, 2010), show that hydrogeologic complexities and large vertical hydraulic gradients can exist within lower permeability rocks within the GBCAAS study area.
- There is the possibility that some areas with high-altitude water-level mounding (shown on plate 2 and figure C–2) beneath mountain blocks may represent perched water levels, rather than the regional potentiometric surface, particularly in areas having low-permeability bedrock that may impede vertical flow. Water levels known to represent perched conditions were not used to develop the potentiometric surface. In contrast, mounding likely occurs beneath other mountain-block areas that are not shown on plate 2 because of the lack of water-level control points (deep wells, springs, perennial streams) to constrain water-table altitudes in these areas. Additional water-level data from deep wells are needed to confirm the extent of regional mounding beneath mountain blocks shown on plate 2.
- While plate 2 delineates five larger shaded areas where potentiometric contours are less certain due to sparsity of water-level data, other smaller areas without water-level data are not delineated, including many mountain blocks without water-level control points that could have groundwater mounding. Water-level mounding in mountain blocks is only shown where there is direct hydrologic evidence (well water levels, spring altitudes, perennial stream altitudes). Water-level mounding likely occurs beneath other mountain blocks within the GBCAAS area and is dependent on recharge and hydraulic conductivity. There is the possibility, therefore, of groundwater mounds not shown on the plate that would divert groundwater flow.
- The estimated total storage volumes of the VU, LBFAU, and UBFAU HGUs are given only for comparison between groundwater flow systems and should not be considered analogous to groundwater availability within the GBCAAS study area.

Summary

The GBCAAS study area has been subdivided into 165 individual HAs and 17 regional groundwater flow systems by previous studies (Harrill and Prudic, 1998, Belcher, 2004). The HAs primarily were based on surface-water divides and range in size from 12 to 4,648 mi^2. The groundwater flow systems were based on directions of interbasin groundwater flow and the location of major discharge areas, and range in size from 282 to 18,849 mi^2. Groundwater flow systems primarily follow surface-water divides.

Groundwater movement in the GBCAAS study area occurs at local, intermediate, and interbasin scales. Within each HA, groundwater typically moves along shallow, short (local scale) or medium (intermediate scale) flow paths, typically from higher altitude areas in the mountains or upper part of the alluvial fan to a nearby stream, spring, or evapotranspiration area. At the interbasin scale, groundwater flows along deeper and longer flow paths between HAs from high-altitude mountains to distant discharge points, often through or around one or more mountain blocks. This interbasin flow typically occurs in areas with hydraulically connected permeable bedrock and where recharge rates in the intervening mountains are relatively small (minimal groundwater mounding). Within the GBCAAS study area, interbasin flow previously had been suggested on the basis of groundwater-budget imbalances (including lack of discharge from some basins), geochemical and isotopic mass-balance studies, and numerical modeling.

A potentiometric-surface map of the GBCAAS study area was constructed for evaluating regional groundwater flow by using water-level data for wells and water-level altitudes for springs and perennial mountain streams. The map illustrates that within each HA, groundwater levels and hydraulic gradients typically follow topographic gradients, but to a lesser degree. Areas with locally steep hydraulic gradients may indicate a decrease in transmissivity or relatively high recharge. At the interbasin scale, groundwater flow between HAs or groundwater flow systems may occur where a gradient exists, higher permeability rocks that permit

groundwater flow comprise the intervening mountains, and substantial groundwater mounding from recharge in the intervening mountains does not occur. The potentiometric-surface map developed for the current study shows water from the central part of Nevada flowing north to the Humboldt River groundwater flow system, northwest to the Great Salt Lake Desert groundwater flow system, or south toward the Death Valley and Colorado River groundwater flow systems. Groundwater from eastern Nevada and western Utah flows east, north, and south towards the Great Salt Lake Desert and Great Salt Lake. Because of averaging of decades of water-level measurements at many wells, the potentiometric-surface map represents an approximate long-term average rather than any specific season or year. This approach is considered appropriate for evaluating regional groundwater flow.

Aquifer geometry and geologic structural features are integral to groundwater flow in the GBCAAS study area. HGUs within the GBCAAS study area often are disrupted by extension; by large-magnitude offset thrust, strike-slip, and normal faults; and by caldera formation; resulting in a complex distribution of rocks. Juxtaposition of thick, low-permeability rock with higher permeability carbonate-rock aquifers by faulting or caldera emplacement commonly forms barriers to groundwater flow and is an important influence on the potentiometric surface. Fault zones themselves may contain low-permeability cores flanked by higher permeability damage zones. These low-permeability fault cores potentially restrict fluid flow across the fault, while the damage zone may conduct groundwater flow parallel to the fault zone.

Regional stratigraphic and structural features within the GBCAAS study area are organized into 14 general subsurface geologic configurations that result in differing likelihoods of hydraulic connection across HA boundaries. For each of these subsurface boundary conditions, the subsurface geologic controls influencing the likelihood of hydraulic connection at HA boundaries were further simplified as (1) low—where low-permeability rocks likely exist at depth and hydraulic connection is unlikely, (2) high—where permeable rocks likely exist at depth and hydraulic connection is permitted by the geologic conditions, or (3) uncertain—where the subsurface geology beneath the boundary or divide is not well constrained and the geologic controls on hydraulic connection are uncertain.

References Cited

Alley, W.M., and Leake, S.A., 2004, The journey from safe yield to sustainability: Ground Water, v. 42 (no. 1), p. 12–16.

Allmendinger, R.W., 1992, Fold and thrust tectonics of the western United States exclusive of the accreted terranes, *in* Burchfiel, B.C., Lipman, P.W., and Zoback, M.L., eds., The Cordilleran orogen: conterminous U.S.: Boulder, Colorado, Geological Society of America, Geology of North America, v. G–3, p. 583–607.

Armstrong, R.L., 1968, Sevier orogenic belt in Nevada and Utah: Geological Society of America Bulletin, v. 79, p. 429–458.

Avery, Charles, 1994, Ground-water hydrology of Ogden Valley and surrounding area, eastern Weber County, Utah, and simulation of ground-water flow in the valley-fill aquifer system: Utah Department of Natural Resources Technical Publication 99, 84 p.

Bedinger, M.S., and Harrill, J.R., 2004, Regional potential for interbasin flow of ground water, Appendix 1, in Belcher, W.R., ed., Death Valley regional ground-water flow system, Nevada and California—Hydrogeologic framework and transient ground-water flow model: U.S. Geological Survey Scientific Investigations Report 2004–5205, p. 355–374.

Belcher, W.R., ed., 2004, Death Valley regional ground-water flow system, Nevada and California—Hydrogeologic framework and transient ground-water flow model: U.S. Geological Survey Scientific Investigations Report 2004–5205, 408 p.

Belcher, W.R., Bedinger, M.S., Back, J.T., and Sweetkind, D.S., 2009, Interbasin flow in the Great Basin with special reference to the southern Funeral Mountains and the source of Furnace Creek springs, Death Valley, California, U.S.: Journal of Hydrology, v. 369, p. 30–43.

Belcher, W.R., Elliot, P.E., and Geldon, A.L., 2001, Hydraulic-property estimates for use with a transient ground-water flow model of the Death Valley regional ground-water flow system, Nevada and California: U.S. Geological Survey Water-Resources Investigations Report 2001–4210, 28 p.

Bjorklund, L.J., Sumsion, C.T., and Sandberg, G.W., 1978, Ground-water resources of the Parowan-Cedar City drainage basin, Iron County, Utah: State of Utah Department of Natural Resources Technical Publication 60, 93 p.

Blakely, R.J., Morin, R.L., McKee, E.H., Schmidt, K.M., Langenheim, V.E., and Dixon, G.L., 1998, Three-dimensional model of pre-Cenozoic basement beneath Amargosa Desert and Pahrump Valley, California and Nevada—Implications for tectonic evolution and water resources: U.S. Geological Survey Open-File Report 98–496, 29 p.

Blankennagel, R.K., and Weir, J.E., Jr., 1973, Geohydrology of the eastern part of Pahute Mesa, Nevada Test Site, Nye County, Nevada: U.S. Geological Survey Professional Paper 712–B, 35 p.

Brooks, L.E., and Mason, J.L., 2005, Hydrology and simulation of ground-water flow in Cedar Valley, Iron County, Utah: U.S. Geological Survey Scientific Investigations Report 2005–5170, 127 p.

Brooks, L.E., and Stolp, B.J., 1995, Hydrology and simulation of ground-water flow in southern Utah and Goshen Valleys, Utah, Utah Department of Natural Resources Technical Publication 111, 96 p.

Burchfiel, B.C., Cowan, D.S., and Davis, G.A., 1992, Tectonic overview of the Cordilleran orogen in the western United States, *in* Burchfiel, B.C., Lipman, P.W., and Zoback, M.L., eds., The Cordilleran orogen: conterminous U.S.: Boulder, Colorado, Geological Society of America, Geology of North America, v. G–3, p. 407–480.

Caine, J.S., Evans, J.P., and Forster, C.B., 1996, Fault zone architecture and permeability structure: Geology, v. 24, p. 1,025–1,028.

Caine, J.S., and Forster, C.B., 1999, Fault zone architecture and fluid flow—Insights from field data and numerical modeling, *in* Haneberg, W.C., Mozley, P.S., Moore, J.C., and Goodwin, L.B., eds., Faults and subsurface fluid flow in the shallow crust: American Geophysical Union Monograph 113, p. 101–127.

Cardinalli, J.L., Roach, L.M., Rush, F.E., and Vasey, B.J., 1968, State of Nevada hydrographic areas, scale 1:500,000, *in* Rush, F.E., ed., Index of hydrographic areas: Nevada Division of Water Resources Information Report 6, 38 p.

Chester, F.M., and Logan, J.M., 1986, Implications for mechanical properties of brittle faults from observations of the Punchbowl fault zones, California: Pure and Applied Geophysics (PAGEOPH), v. 124, p. 79–106.

Coney, P.J., 1980, Cordilleran metamorphic core complexes, *in* Crittenden, M.D., Coney, P.J., and Davis, G.H., eds., Cordilleran metamorphic core complexes: Geological Society of America Memoir 153, Geological Society of America, Boulder, Colorado, p. 7–34.

Coplen, T.B., Winograd, I.J., Landwehr, J.M., and Riggs, A.C., 1994, 500,000-year stable carbon isotopic record from Devils Hole, Nevada: Science, v. 263, p. 361–365.

Cordova, R.M., 1970, Ground-water conditions in southern Utah Valley and Goshen Valley, Utah: Utah Department of Natural Resources Technical Publication 28, 79 p.

D'Agnese, F.A., Faunt, C.C., Turner, A.K., and Hill, M.C., 1997, Hydrogeologic evaluation and numerical simulation of the Death Valley regional ground-water flow system, Nevada, and California: U.S. Geological Survey Water-Resources Investigations Report 1996–4300, 124 p.

DeCelles, P.G., 2004, Late Jurassic to Eocene evolution of the Cordilleran thrust belt and foreland basin system, western USA: American Journal of Science, v. 304, p. 105–168.

Dettinger, M.D., 1989, Distribution of carbonate-rock aquifers in southern Nevada and the potential for their development—Summary of findings, 1985–88: Carson City, Nev., State of Nevada, Program for the Study and Testing of Carbonate-Rock Aquifers in Eastern and Southern Nevada, Summary Report no. 1, 37 p.

Dettinger, M.D., Harrill, J.R., Schmidt, D.L., and Hess, J.W., 1995, Distribution of carbonate-rock aquifers and the potential for their development, southern Nevada and parts of Arizona, California, and Utah: U.S. Geological Survey Water–Resources Investigations Report 91–4146, 100 p.

Dettinger, M.D., and Schaefer, D.H., 1996, Hydrogeology of structurally extended terrain in the eastern Great Basin of Nevada, Utah, and adjacent states, from geologic and geophysical models: U.S. Geological Survey Hydrologic Investigations Atlas HA–694–D, 1 sheet, scale 1:15,000,000.

Dudley, W.W., Jr., and Larsen, J.D., 1976, Effect of irrigation pumping on desert pupfish habitats in Ash Meadows, Nye County, Nevada: U.S. Geological Survey Professional Paper 927, p. 1–52.

Ekren, E.B., Bucknam, R.C., Carr, W.J., Dixon, G.L., and Quinlivan, W.D., 1976, East-trending structural lineaments in central Nevada: U.S. Geological Survey Professional Paper 986, 16 p., 1 pl. in pocket.

Elliot, P.E., Beck, D.A., and Prudic, D.E., 2006, Characterization of surface-water resources in the Great Basin National Park area and their susceptibility to ground-water withdrawals in adjacent valleys, White Pine County, Nevada: U.S. Geological Survey Scientific Investigations Report 2006–5099, 156 p.

Emsbo, Poul, Groves D.I., Hofstra A.H., and Bierlein, F.P., 2006, The giant Carlin gold province – A protracted interplay of orogenic, basinal, and hydrothermal processes above a lithospheric boundary: Mineralium Deposita, v. 41, p. 517–525.

Fenelon, J.M., Sweetkind, D.S., and Laczniak, R.J., 2010, Groundwater flow systems at the Nevada Test Site, Nevada: A synthesis of potentiometric contours, hydrostratigraphy, and geologic structures: U.S. Geological Survey Professional Paper 1771, 54 p., 6 pls.

Fetter, C.W., 1980, Applied hydrogeology: Charles E. Merrill Publishing Company, Columbus, Ohio, 488 p.

Folch, Albert, and Mas-Pla, Josep, 2008, Hydrogeological interactions between fault zones and alluvial aquifers in regional flow systems: Hydrological Processes v. 22, p. 3,476–3,487.

Freeze, R.A., and Cherry, J.A., 1979, Groundwater: Englewood Cliffs, New Jersey, Prentice-Hall, 604 p.

Gans, P.B., and Miller, E.L., 1983, Styles of mid-Tertiary extension in east-central Nevada, *in* Gurgel, K.D., ed., Geologic excursions in the overthrust belt and metamorphic core complexes of the intermountain region, Nevada: Utah Geological and Mineral Survey Special Studies 59, p. 107–160.

Gates, J.S., and Kruer, S.A., 1981, Hydrologic reconnaissance of the southern Great Salt Lake Desert and summary of the hydrology of west-central Utah: State of Utah Department of Natural Resources Technical Publication 71, 55 p.

Gleeson, Tom, and Manning, A.H., 2008, Regional groundwater flow in mountainous terrain: Three-dimensional simulations of topographic and hydrogeologic controls: Water Resources Research, v. 44, 16 p.W10403, doi:10.1029/2008WR006848, accessed December 22, 2008 at http://www.agu.org/pubs/crossref/2008/2008WR006848.shtml.

Hamilton, W.B., 1988, Detachment faulting in the Death Valley region, California and Nevada, *in* Carr, M.D., and Yount, J.C., eds., Geologic and hydrologic investigations of a potential nuclear waste disposal site at Yucca Mountain, southern Nevada: U.S. Geological Survey Bulletin 1790, p. 51–85.

Harrill, J.R., 1982, Ground-water storage depletion in Pahrump Valley, Nevada-California, 1962–75: U.S. Geological Survey Water-Supply Paper 2279, 53 p.

Harrill, J.R., Gates, J.S., and Thomas, J.M., 1988, Major ground-water flow systems in the Great Basin region of Nevada, Utah, and adjacent states: U.S. Geological Survey Hydrologic Investigations Atlas HA–694–C, 2 sheets, scale 1:1,000,000.

Harrill, J.R. and Prudic, D.E., 1998, Aquifer systems in the Great Basin region of Nevada, Utah, and adjacent states—Summary report: U.S. Geological Survey Professional Paper 1409–A, 66 p.

Holmes, W.F., and Thiros, S.A., 1990, Ground-water hydrology of the Pahvant Valley and adjacent areas, Utah: Utah Department of Natural Resources Technical Publication 98, 64 p.

Hofstra, A.H., and Cline, J.S., 2000, Characteristics and models for Carlin-type gold deposits: Reviews in Economic Geology, v. 13, p. 163–220.

Hood, J.W., and Waddell, K.M., 1969, Hydrologic reconnaissance of Deep Creek Valley, Tooele and Juab Counties, Utah and Elko and White Pine Counties, Nevada: State of Utah Department of Natural Resources Technical Publication 24, 54 p.

Kariya, K.A., Roark, D.M., Hanson, K.M., 1994, Hydrology of Cache Valley, Cache County, Utah, and adjacent part of Idaho, with emphasis on simulation of ground-water flow, Utah Department of Natural Resources Technical Publication 108, 120 p.

Kirk, S.T., and Campana, M.E., 1990, A deuterium-calibrated groundwater flow model of a regional carbonate-alluvial system: Journal of Hydrology, v. 119, p. 357–388.

Lambert, P.M., 1995, Numerical simulation of ground-water flow in basin-fill material in Salt Lake Valley, Utah: Utah Department of Natural Resources Technical Publication 110–B, 58 p.

Langenheim, V.E., Grow, J.A., Jachens, R.C., Dixon, G.L., and Miller, J.J., 2001, Geophysical constraints on the location and geometry of the Las Vegas Valley shear zone, Nevada: Tectonics, v. 20, p. 189–209.

Lipman, P.W., 1984, The roots of ash flow calderas in western North America—windows into the tops of granitic batholiths: Journal of Geophysical Research, v. 89, p. 8,801–8,841.

Luckey, R.R., Tucci, Patrick, Faunt, C.C., Ervin, E.M., Steinkampf, W.C., D'Agnese, F.A., and Patterson, G.L., 1996, Status of understanding of the saturated-zone ground-water flow system at Yucca Mountain, Nevada, as of 1995: U.S. Geological Survey Water-Resources Investigations Report 96–4077, 71 p.

Lundmark, K.W., 2007, Regional water budget accounting and uncertainty analysis model using a deuterium-calibrated discrete state compartment model: White Pine County, Nevada and adjacent areas in Nevada and Utah: Reno, University of Nevada, M.S. thesis, 177 p.

Manning, A.H., and Caine, J.S., 2007, Groundwater noble gas, age, and temperature signatures in an alpine watershed: Valuable tools in conceptual model development: Water Resources Research, v. 43, W04404, 16 p., doi:10.1029/2006WR005349, accessed November 6, 2008 at http://www.agu.org/pubs/crossref/2007/2006WR005349.shtml.

Mathey, Sharon B., ed., 1998, National Water Information System (NWIS): U.S. Geological Survey Fact Sheet 027–98, 2 p., accessed January 14, 2009 at http://pubs.usgs.gov/fs/FS-027-98/fs-027-98.pdf.

McKee, E.H., Wickham, T.A., and Wheeler, K.L., 1998, Evaluation of faults and their effect on ground-water flow southwest of Frenchman Flat, Nye and Clark Counties, Nevada—A digital database: U.S. Geological Survey Open-File Report 98–580, 16 p., 4 plates.

Mower, R.W., 1982, Hydrology of the Beryl-Enterprise Area, Escalante Desert, Utah, with emphasis on ground water: Utah Department of Natural Resources Technical Publication 73, 66 p.

Mower, R.W., and Cordova, R.M., 1974, Water resources of the Milford area, Utah, with emphasis on ground water: Utah Department of Natural Resources Technical Publication 43, 106 p.

Potter, C.J., Sweetkind, D.S., Dickerson, R.P., and Killgore, M.L., 2002, Hydrostructural maps of the Death Valley regional flow system, Nevada and California, version 1.0: U.S. Geological Survey Miscellaneous Field Studies Map MF–2372, 2 sheets, scale 1:350,000, with pamphlet.

PRISM Climate Group, Oregon State University, 2007, Digital climate data, accessed May 2, 2007, at http://www.ocs.oregonstate.edu/prism/index.phtml.

Prudic, D.E., Harrill, J.R., and Burbey, T.J., 1995, Conceptual evaluation of regional ground-water flow in the Carbonate-Rock Province of the Great Basin, Nevada, Utah, and adjacent states: U.S. Geological Survey Professional Paper 1409–D, 102 p.

Rowley, P.D., 1998, Cenozoic transverse zones and igneous belts in the Great Basin, western United States—Their tectonic and economic implications, *in* Faulds, J.E., and Stewart, J.H., eds., Accommodation zones and transfer zones; The regional segmentation of the Basin and Range province: Geological Society of America Special Paper 323, p. 195–228.

Rush, F.E., 1968, Index of hydrographic areas in Nevada: Nevada Division of Water Resources Information Report 6, 38 p.

Smith, D.L., Gans, P.B., and Miller, E.L., 1991, Palinspastic restoration of Cenozoic extension in the central and eastern Basin and Range province at latitude 39–40 degrees N, *in* Geology and ore deposits of the Great Basin, Reno NV: Geological Society of Nevada Symposium Proceedings, p. 75–86.

Smith, R.L., and Bailey, R.A., 1968, Resurgent calderas: Geological Society of America Memoir 116, p. 613–662.

Steinkampf, W.C., and Werrell, W.L., 2001, Ground-water flow to Death Valley as inferred from the chemistry and geohydrology of selected springs in Death Valley National Park, California and Nevada: U.S. Geological Survey Water-Resources Investigations Report 98–4114, 37 p.

Stephens, J.C., 1974, Hydrologic reconnaissance of the northern Great Salt Lake Desert and summary hydrologic reconnaissance of northwestern Utah: State of Utah Department of Natural Resources Technical Publication 42, 55 p.

Stewart, J.H., 1998, Regional characteristics, tilt domains, and extensional history of the later Cenozoic Basin and Range province, western North America, *in* Faulds, J.E., and Stewart, J.H., eds., Accommodation zones and transfer zones, the regional segmentation of the Basin and Range Province: Geological Society of America Special Paper 323, p. 47–74.

Sweetkind, D.S., Belcher, W.R., Faunt, C.C., and Potter, C.J., 2004, Geology and hydrogeology, Chap. B of Belcher, W.R., ed., 2004, Death Valley regional ground-water flow system, Nevada and California—Hydrogeologic framework and transient ground-water flow model: U.S. Geological Survey Scientific Investigations Series Report 1171, p. 21–98.

Thiros, S.A., Stolp, B.J., Hadley, H.K., and Steiger, J.I., 1996, Hydrology and simulation of ground-water flow in Juab Valley, Juab County, Utah: Utah Department of Natural Resources Technical Publication 114, 100 p.

Thomas, J.M., Calhoun, S.C., and Apambire, W.B., 2001, A deuterium mass-balance interpretation of groundwater sources and flows in southeastern Nevada: Desert Research Institute Publication no. 41169, p. 46.

Thomas, J.M., Mason, J.L., and Crabtree, J.D., 1986, Ground-water levels in the Great Basin region of Nevada, Utah, and adjacent states: U.S. Geological Survey Hydrologic Investigations Atlas HA–694–B, 2 sheets.

Thyne, G.D., Gillespie, J.M., and Ostdick, J.R, 1999, Evidence for interbasin flow through bedrock in the southeastern Sierra Nevada: Geological Society of America Bulletin, v. 111, p. 1,600–1,616.

Tiedeman, C.R., Goode, D.J., and Hseih, P.A., 1998, Characterizing a ground water basin in a New England mountain and valley terrain: Ground Water, v. 36, no. 4, p. 611–620.

Toth, Jozsef, 1963, A theoretical analysis of groundwater flow in small drainage basins: Journal of Geophysical Research, v. 68, no. 8, p. 2,354–2,356, doi:10.1029/JZ068i008p02354, accessed October 31, 2008 at http://www.agu.org/journals/jz/v068/i008/JZ068i008p02354/.

U.S. Geological Survey EROS Data Center, 1999, 1 arc-second (30-meter) National Elevation Dataset: U.S. Geological Survey dataset, accessed September 15, 2008 at http://ned.usgs.gov/.

U.S. Geological Survey, 1999, National Hydrography Dataset: U.S. Geological Survey Fact Sheet 106–99, accessed March 2007 at http://erg.usgs.gov/isb/pubs/factsheets/fs10699.html.

Welch, A.H., Bright, D.J., and Knochenmus, L.A., eds., 2007, Water resources of the Basin and Range carbonate-rock aquifer system, White Pine County, Nevada, and adjacent areas in Nevada and Utah: U.S. Geological Survey Scientific Investigations Report 2007–5261, 96 p.

Wernicke, B.P., 1992, Cenozoic extensional tectonics of the U.S. Cordillera, *in* Burchfiel, B.C., Lipman, P.W., and Zoback, M.L., eds., The Cordilleran orogen: conterminous U.S.: Boulder, Colorado, Geological Society of America, Geology of North America, v. G–3, p. 553–581.

Wernicke, B.P., Guth, P.L., and Axen, G.J., 1984, Tertiary extensional tectonics in the Sevier thrust belt of southern Nevada, *in* Lintz, J.P., ed., Western geological excursions: Mackay School of Mines, Reno, University of Nevada, Geological Society of America, Cordilleran Section, Field Trip Guidebook, p. 473–510.

Wilson, J.W., 2007, Water-level surface maps of the carbonate-rock and basin-fill aquifers in the Basin and Range carbonate-rock aquifer system, White Pine County, Nevada, and adjacent areas in Nevada and Utah: U.S. Geological Survey Scientific Investigations Report 2007–5089, 10 p., 2 pls.

Winograd, I.J., and Pearson, F.J., 1976, Major carbon 14 anomaly in a regional carbonate aquifer: possible evidence for megascale channeling, south central Great Basin: Water Resources Research, v. 12, p. 1,125–1,143.

Winograd, I.J., and Thordarson, W., 1975, Hydrogeologic and hydrochemical framework, south-central Great Basin, Nevada-California, with special reference to the Nevada Test Site: U.S. Geological Survey Professional Paper 712–C, 126 p.